



High Efficiency Organic Solar Cells

December 16, 2009 — February 2, 2011

Kenneth Walker and Steven Joslin
Luna Innovations, Inc.
Danville, Virginia

NREL is a national laboratory of the U.S. Department of Energy, Office of Energy Efficiency & Renewable Energy, operated by the Alliance for Sustainable Energy, LLC.

Subcontract Report
NREL/SR-5200-51382
May 2011

Contract No. DE-AC36-08GO28308

High Efficiency Organic Solar Cells

December 16, 2009 — February 2, 2011

Kenneth Walker and Steven Joslin
Luna Innovations, Inc.
Danville, Virginia

NREL Technical Monitor: Brian Keyes
Prepared under Subcontract No. NEU-0-99010-08

NREL is a national laboratory of the U.S. Department of Energy, Office of Energy Efficiency & Renewable Energy, operated by the Alliance for Sustainable Energy, LLC.

**This publication was reproduced from the best available copy
submitted by the subcontractor and received no editorial review at NREL.**

NOTICE

This report was prepared as an account of work sponsored by an agency of the United States government. Neither the United States government nor any agency thereof, nor any of their employees, makes any warranty, express or implied, or assumes any legal liability or responsibility for the accuracy, completeness, or usefulness of any information, apparatus, product, or process disclosed, or represents that its use would not infringe privately owned rights. Reference herein to any specific commercial product, process, or service by trade name, trademark, manufacturer, or otherwise does not necessarily constitute or imply its endorsement, recommendation, or favoring by the United States government or any agency thereof. The views and opinions of authors expressed herein do not necessarily state or reflect those of the United States government or any agency thereof.

Available electronically at <http://www.osti.gov/bridge>

Available for a processing fee to U.S. Department of Energy
and its contractors, in paper, from:

U.S. Department of Energy
Office of Scientific and Technical Information

P.O. Box 62
Oak Ridge, TN 37831-0062
phone: 865.576.8401
fax: 865.576.5728
email: <mailto:reports@adonis.osti.gov>

Available for sale to the public, in paper, from:

U.S. Department of Commerce
National Technical Information Service
5285 Port Royal Road
Springfield, VA 22161
phone: 800.553.6847
fax: 703.605.6900
email: orders@ntis.fedworld.gov
online ordering: <http://www.ntis.gov/help/ordermethods.aspx>

Cover Photos: (left to right) PIX 16416, PIX 17423, PIX 16560, PIX 17613, PIX 17436, PIX 17721



Printed on paper containing at least 50% wastepaper, including 10% post consumer waste.

Table of Contents

Table of Contents	4
High Efficiency Organic Solar Cells Program Summary	5
Deliverable #1: Baseline Performance >4.5% PCE	6
Deliverable #2: Demonstrate V_{oc} Advantage of at least 250mV	8
Deliverable #3: Demonstration of >7% PCE	10
Blend Ratio	10
Spin Coating and Thermal Treatment	12
Spin Coating.....	12
Additives	12
Cathode Material	12
Device Fabrication and Characterization	17
Thermal Annealing.....	20
Film Morphology and AFM	21
Photoluminescence Spectroscopy.....	25
Additional Derivatives Tested as Acceptors	30
Synthetic approach to develop a library of novel OPV acceptor materials.....	32
Synthesis of C_{70} and TMS derivatives with desired electronic properties	32
Acceptor materials based on Trimetaspheres	32
New TMS derivatives of the PCBX type.....	35
TMS derivatives with new linkers	36
Acceptor materials based on empty cage fullerenes	38
Additional Polymers Tested as Donors with Lu-PCBEH	43
Conclusions.....	44

High Efficiency Organic Solar Cells Program Summary

Program accomplishments include certification of an open circuit voltage increase of more than 250mV over a C₆₀-PCBM baseline device using low band gap polymer, verification of HOMO/LUMO levels for six low band gap polymer samples from Plextronics Incorporated, synthesis of eight new acceptor molecules, device fabrication and testing of blends for all Plextronics' polymers plus an additional three polymers from the University of North Carolina – Chapel Hill, 2cm² device fabrication and testing at Plextronics, and future test plans for OPV acceptor development.

During the performance of this program, a significant gap in the literature was discovered regarding inconsistency of reported HOMO/LUMO energy levels as measured by electrochemistry (EC) over the past decade or more. The discrepancies arise from errors associated with conversion of raw EC data to vacuum level energies. Specific details have been submitted for publication in *Advanced Materials* under the title: *Electrochemical Considerations for Determining Absolute Frontier Orbital Energy Levels of Conjugated Polymers for Solar Cell Applications* (Claudia M. Cardona, Wei Li, Angel E. Kaifer, David Stockdale, Guillermo C. Bazan). The manuscript is attached as Appendix A.

In general, the results of this program clearly show an open circuit voltage (V_{oc}) advantage of over 250mV for the Trimetasphere (TMS) based acceptor compared to baseline C₆₀-PCBM. However, an energy transfer or charge trap mechanism has so far prevented generation of the closed circuit current (I_{sc}) necessary for improvement in overall power conversion efficiency (PCE). Considerable support was provided by NREL to study potential causes for the observed low current associated with the polymers available for testing during the program. It is important to note that Trimetasphere based acceptors have demonstrated equivalent I_{sc} compared to C₆₀-PCBM when blended with P3HT. Tests performed at NREL point to low charge transfer rates for the low band gap polymer/TMS blends evaluated. However, the reasons for this were not clear based on the limited testing performed. It is possible that the HOMO/LUMO levels are unsuitable for efficient charge separation or that the structure of the polymer is incompatible with that of the acceptor such that the fullerene cannot physically engage the polymer in a manner necessary for charge transfer, for example due to steric hindrance. Further development is required to fully understand and subsequently modify either the polymer or acceptor to overcome this problem. Such a program has been proposed along with letters of support from across the commercial and academic OPV community.

The results are presented in three sections based on the deliverables of the program. First, baseline performance for Lu-PCBEH acceptor blended with P3HT was demonstrated at **4.89% PCE exceeding the 4.5% PCE goal**. Second, an increase of over 250mV in V_{oc} was demonstrated for Lu-PCBEH blended with low band gap polymers compared to a comparable C₆₀-PCBM device. **The actual V_{oc} was certified at 260mV higher for a low band gap polymer device using the Lu-PCBEH acceptor.** Finally, the majority of the effort was focused on development of a device with over 7% PCE. While low current and fill factors suppressed overall device performance for the low band gap polymers tested, significant discoveries were made that point the way for future development of these novel acceptor materials.

Deliverable #1: Baseline Performance >4.5% PCE

Baseline performance exceeded expectations by demonstrating 4.89% PCE for a P3HT/Lu-PCBEH blend device. Initial devices fell short of the required baseline performance due to degradation during shipping to NREL for certification. Subsequent changes to device preparation and shipping materials brought internal measurements in line with NREL certification data. Discussions with NREL Certification Lab staff were extremely helpful in resolving the shipping degradation problem.

Initial baseline devices prepared at Luna tested internally at over 4.8% conversion efficiency. However, results at the Certification Laboratory were substantially lower with the best device measuring 4.3%. Of the many potential causes for the difference in measured conversion efficiency, the most likely included calibration of Luna's test equipment and degradation during shipment.

Historically, Luna's test equipment and process have provided excellent agreement with the certification lab at NREL. Luna's silicon reference cell was tested at NREL prior to delivery in 2005. Luna uses a KG3 filter for the solar simulator. To test stability of the reference cell, recently measured data is overlaid on the original data in Figure 1. The recent data shows the reference cell has remained stable from 2005 to date. In 2008, Luna obtained a certification from NREL for a 0.06cm^2 device with an efficiency of 4.51%. The same test protocol was used for the devices submitted for certification during this program. Device degradation during shipment is therefore the most likely cause for the observed difference in performance.

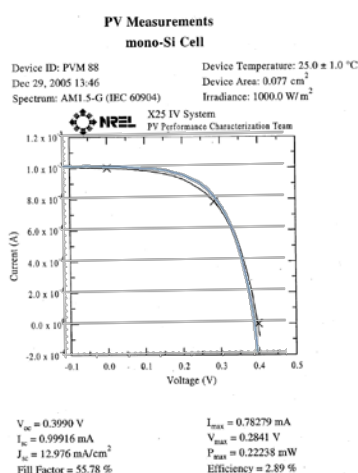


Figure 1: Comparison of initial calibration file from 2005 to recent data (blue).

Root cause analysis required testing of shipping materials and device stability. Devices stored for over 45 days in an argon glove box showed no significant degradation in performance.

Therefore, contamination or loss of inert atmosphere was suspected as the most likely reason for degradation. To determine the root cause, Luna fabricated and tested a number of devices exposed to different shipping conditions including

devices packed identical to those shipped for certification (using foam), packed using bubble wrap in place of the foam as well as a device exposed to air.

The data indicate exposure to air best matches the mode of degradation observed for the samples submitted for the baseline performance deliverable. The difference in measured performance between typical Luna and NREL data is shown in Figure 2. Significant performance degradation is not noted until over 29 hours of exposure to air. Hence the most likely cause is the loss of inert atmosphere during shipment from Luna to NREL.

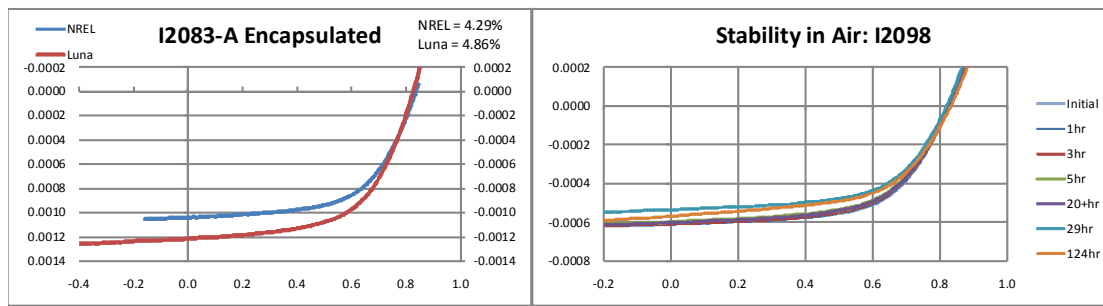


Figure 2: Device data taken at Luna and NREL (left) showing loss of current that appears similar to that found upon exposure to air at Luna (right). Loss of inert atmosphere during shipment is suspected as the root cause for discrepancy between Luna and NREL performance data.

Data for other exposure tests are shown in Figure 3, including bubble wrap and foam shipping materials. An initial thought was that the foam material had absorbed oxygen or water that contaminated the shipping container. However, the sample packed identically to those shipped for certification showed a decrease in fill factor with minimal change in current whereas the actual samples shipped to NREL showed primarily a loss of current.

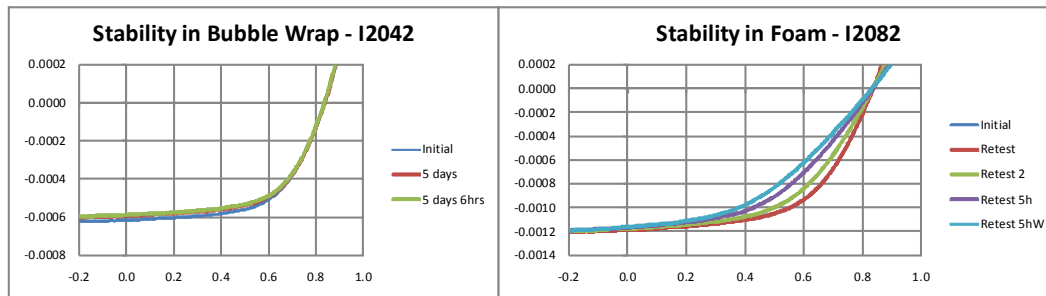


Figure 3: Device degradation due to exposure to bubble wrap and foam packing materials. Each device was placed inside a sealed plastic bag and then into the stainless steel shipping tube. Samples were removed for testing and re-packed.

New baseline devices were fabricated that subsequently exceeded the 4.5% PCE requirement for the deliverable. These devices included several significant changes that were intended to improve device stability. First, the silver paint was applied after encapsulation to remove the potential for oxygen and moisture penetration between the epoxy and silver paint to the backside aluminum electrode. A desiccant was applied to the cover slide to help protect the backside electrodes. The backside electrodes were increased in thickness from 100nm to 170nm. A significant increase in current was required to deposit the thicker aluminum which effectively limited the electrode to 170nm.

Alternative contact materials were tested. Copper foil with a conductive adhesive performed worse than silver paint. Retesting after one week showed complete loss of contact between the copper foil and device. Indium and silver paste in place of silver paint for the backside electrode contacts were also evaluated with no improvement relative to silver paint.

In addition to the device changes mentioned previously, Plextronics delivered one gram of Plexcore 2000, a P3HT-based polymer, for comparison to the Rieke P3HT polymer. Initial testing showed slightly lower performance for Plexcore. Therefore the baseline device was made with P3HT from Rieke Metals, Inc. **The resulting baseline device successfully met the deliverable goal with PCE certified at 4.89%.** Actual performance data is shown in Figure 4.

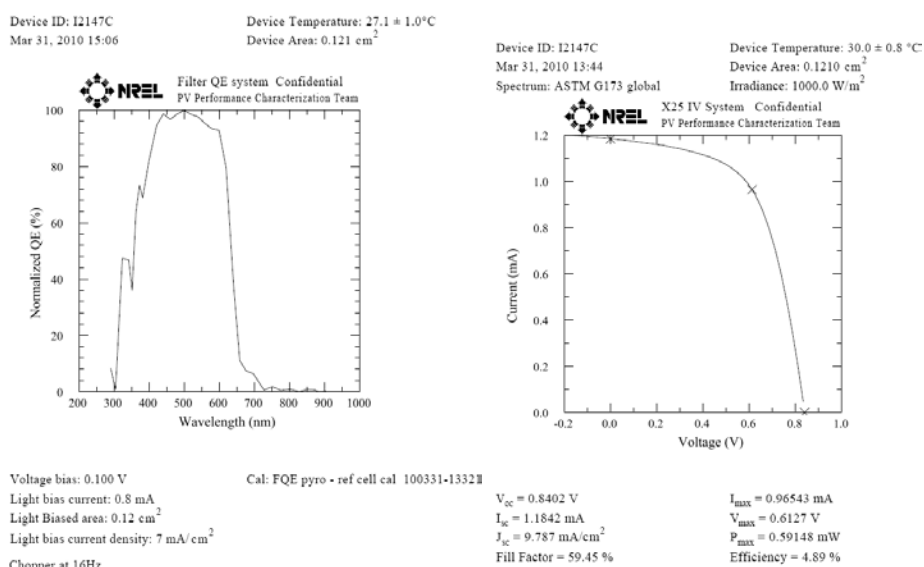


Figure 4: NREL certification of 4.89% baseline device performance. The device was made with P3HT from Rieke Metals and Lu-PCBEH.

Deliverable #2: Demonstrate V_{oc} Advantage of at least 250mV

The basis for improved PCE using Trimetasphere based acceptors is the resulting improvement in V_{oc} . Baseline devices used a blend of Lu-PCBEH/P3HT which delivered 280mV higher V_{oc} compared to C_{60} -PCBM/P3HT blend. The second deliverable was therefore to demonstrate an improvement of over 250mV in open circuit voltage for Lu-PCBEH when blended with a low band gap polymer. Several low band gap polymers were evaluated. In nearly every case, the measured device performance confirmed an improvement in V_{oc} for Lu-PCBEH compared to C_{60} -PCBM when blended with a range of low band gap polymers.

Plextronics delivered 100mg each of two donor polymers, Plex A and Plex B. Initial testing with Lu-PCBEH confirmed an increase in V_{oc} compared to C_{60} -PCBM by 260mV for the Plex A polymer. The J-V characteristics of this polymer combined with Lu-PCBEH and C_{60} -PCBM are shown in Figure 5. Integrated EQE data for the Plex A/ C_{60} -PCBM device gave a current within 1% of the measured current. However, EQE data for the Lu-PCBEH device differed from the measured current by more than 20%, Figure 6. This variation was attributed to differences in morphology between devices, which are known to significantly influence device performance. **The second deliverable was made using a blend of Plex A polymer/Lu-PCBEH acceptor which demonstrated a 260mV advantage compared to a baseline Plex A/ C_{60} -PCBM device.** However, device performance was low at 0.26% PCE due to low current and fill factor.

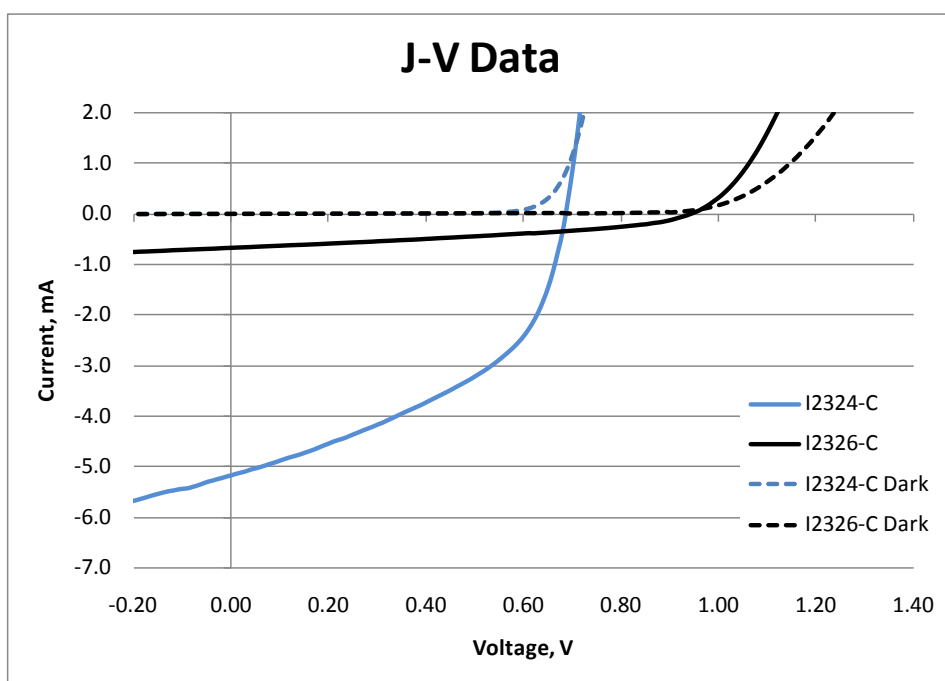


Figure 5: Current vs. voltage for Plex A devices. I2324 is Plex A/C₆₀-PCBM, I2326 is Plex A/Lu-PCBEH

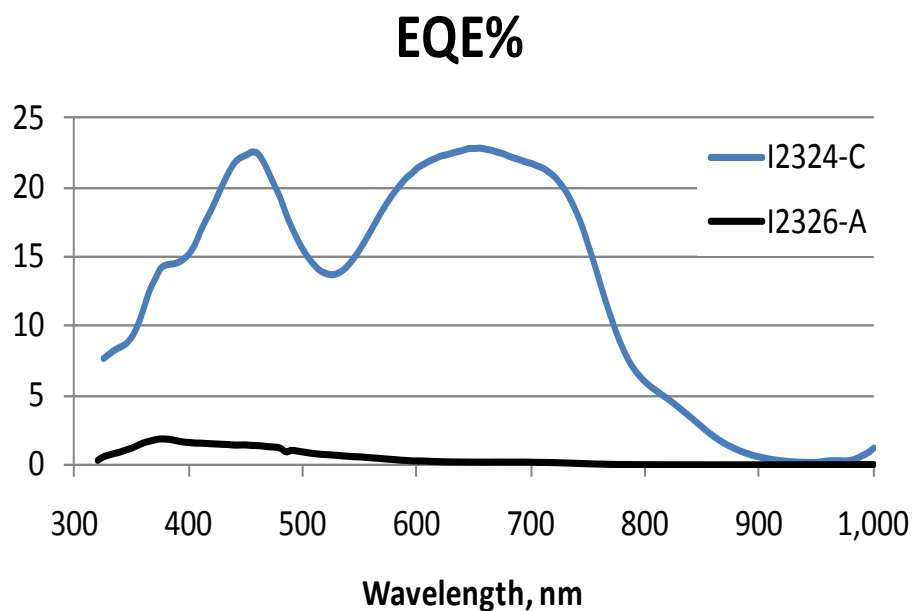


Figure 6: EQE data for Plex A devices, I2324 with C60-PCBM and I2326 with Lu-PCBEH.

Deliverable #3: Demonstration of >7% PCE

The device performance for blends using the Lu-PCBEH acceptor molecule was expected to require substantial optimization of morphology. Process modifications included blend ratio, solvent variations – including additives or orthogonal solvents, spin coating conditions, and thermal annealing conditions. Performance varied depending on the parameters used to fabricate each device. In addition to processing conditions, the size difference between acceptor molecules was expected to have significant influence regarding morphology development of the active layer. The C₈₀ cage of Lu-PCBEH is much larger than the C₆₀ cage of the typical PCBM acceptor.

For Plex A, performance improved significantly with the addition of 1,8 diiodooctane (4%) in *o*-dichlorobenzene (ODCB) for all parameters, Table 1. Results of Plex A testing was more stable using ODCB compared to chlorobenzene (CB). However, device efficiency remained low at ~0.27% on average. Plex B was more soluble in CB compared to ODCB and therefore initial testing was done only in chlorobenzene solutions with and without additives. For the Plex B blends with Lu-PCBEH, using 1,8-Diiodooctane (DIO) additive in CB provided significant improvement in V_{oc} compared to CB or CB with 2% chloronaphthalene additive. However, lower current and fill factor yielded PCE <0.1%. No degradation was observed after aging 20 days in argon. However, device efficiency remained low at ~0.25% on average for Plex A blends, Table 2.

Further testing of Plex A and Plex B included variations in blend ratio, concentration, and solvent additives with the objective of improving active layer morphology. The solubility of Plex B material in combination with Lu-PCBEH was insufficient for good film deposition under any of the deposition conditions attempted. Limited data for Plex B/Lu-PCBEH showed wide variation with V_{oc} ranging from 0 to 910mV, J_{sc} ranging from 0 to 0.25mA and fill factors in the range of 25% to 34%. Solutions of 10:30 (polymer:acceptor in mg/ml ODCB) clogged a 1μm filter after extended stirring at 70°C. Even after filtration, particles were observed in most films causing comet tails and starbursts during spin coating and drying, respectively.

Work was therefore focused on Plex A material paired with either C₇₀-PCBM or Lu-PCBEH to compare the process conditions necessary for good performance using Plex A polymer. The initial blend ratio was 10:10 mg/ml. A calcium/aluminum cathode was deposited at 10nm/190nm thickness based on Plextronics' preference for Ca instead of LiF. Typically Plex A/C₇₀-PCBM produces device performance of about 3.5% PCE when processed at Plextronics. However, differences in processing equipment often lead to variation in process conditions. Therefore, using C₇₀-PCBM from Nano-C, devices were made to correlate processing conditions at Luna to those used at Plextronics for a known active layer system.

Blend Ratio

Changes in blend ratio and solvent annealing alone (highlighted in Table 3) provided an increase in V_{oc}, but little improvement in overall PCE performance. Additives were by far the most effective means to improve performance. Additional testing of additive concentration is discussed later in this report.

Table 1: Device fabrication conditions and performance results summary

Polymer	Acceptor	Ratio	Solvent	Additive	PCE, %	V _{oc} , mV	J _{sc} , mA	FF
Plexcore	C ₆₀ -PCBM	10:10	CB	2% ClNp	2.13	520	7.06	0.58
Plex A	C ₆₀ -PCBM	10:10	ODCB	4% DIO	1.55	680	5.02	0.45
Plex A	Lu-PCBEH	10:10	ODCB	---	0.04	342	0.414	0.26
Plex A	Lu-PCBEH	10:10	ODCB	4% DIO	0.26	940	0.710	0.38
Plex A	Lu-PCBEH	12:15	ODCB	---	0.06	610	0.286	0.33
Plex A	Lu-PCBEH	15:12	ODCB	---	0.06	694	0.282	0.30
Plex A	Lu-PCBEH	10:10	ODCB	4% DIO	0.19	710	0.908	0.29
Plex B	Lu-PCBEH	10:8	CB	---	0.001	25	0.148	0.27
Plex B	Lu-PCBEH	5:10	CB	---	0.001	26	0.220	0.25
Plex B	Lu-PCBEH	8:8	CB	2% ClNp	0.002	46	0.190	0.24
Plex B	Lu-PCBEH	10:10	CB	4% DIO	0.007	168	0.140	0.28

Table 2: V_{oc} comparison between C₆₀-PCBM and Lu-PCBEH paired with Plex A.

Polymer	Acceptor	Ratio	Solvent	Additive	PCE, %	V _{oc} , mV	J _{sc} , mA	FF
Plex A	C60-PCBM	10:10	ODCB	DIO 4%	1.22	680	3.86	0.46
Plex A*	C60-PCBM	10:10	ODCB	DIO 4%	1.21	690	3.83	0.46
Plex A	C60-PCBM	10:10	ODCB	DIO 4%	1.60	690	5.16	0.45
Plex A	Lu-PCBEH	10:10	ODCB	DIO 4%	0.25	940	0.69	0.39
Plex A	Lu-PCBEH	10:10	ODCB	DIO 4%	0.25	950	0.686	0.39
Plex A	Lu-PCBEH	10:10	ODCB	DIO 4%	0.23	940	0.694	0.35

* Re-measured after 20 days in glove box

Spin Coating and Thermal Treatment

A matrix of spin coating and thermal treatment conditions was tested. However, the best Plex A/C₇₀-PCBM device fabricated at Luna provided only 1.56% PCE. Spin speed and time, drying conditions, as well as thermal annealing temperature and time were varied with limited impact on device performance. After spin coating, samples were dried in either an open or closed Petri dish (PD). Open circuit voltage was consistent at 670mV, similar to results for C₆₀-PCBM. Results are shown in Table 4. Post-annealing conditions were explored as a means to improve short circuit current, Table 5. However, post annealing proved to be insufficient to match the performance of this system at Plextronics. In addition to variability from equipment differences, the purity of the C₇₀-PCBM is a potential cause for low performance.

Spin Coating

Another matrix of Plex A/C₇₀-PCBM devices was planned using a blend ratio of 10:10 mg/ml in ODCB with no additives or thermal treatments to more directly explore the impact of spin conditions. The data in Table 6 indicate the best performance is produced by spin coating at 700rpm for 100sec. A similar set of devices were made using a 10:10, Plex A:Lu-PCBEH blend, again with no additive or thermal treatment. To date, the best device was obtained by spin coating at 600rpm for 150sec, Table 7.

Additives

The use of additives was investigated for 1,8 diiodooctane (DIO) and 1,8 octanedithiol (ODT) in ODCB. The amount of additive used was varied as well as spin coating and thermal treatment conditions. The results are shown in Table 8. Clearly the use of DIO improved and stabilized V_{oc} of the Plex A/Lu-PCBEH blend devices. Increasing the amount of additive improved the fill factor and short circuit current as well. This observation is in contrast to experience at Plextronics where the best performance (3.5% with C₇₀-PCBM) was obtained without an additive.

Cathode Material

Calcium/aluminum and lithium fluoride/aluminum cathodes were compared using P3HT/Lu-PCBEH blend devices. Results indicate an advantage for LiF/Al over Ca/Al in terms of V_{oc} (820 vs. 700mV), J_{sc} (10.1 vs. 9.6 mA/cm²) and PCE (4.97% vs. 4.18%).

Table 3: Effect of blend ratio and solvent system on device performance

Donor	Acceptor	Ratio	Solvent	Additive	Data			
					Voc	Jsc	FF	Eff
Plex A	C ₇₀ -PCBM	10:10	ODCB	None	0.60	5.98	0.33	1.19
	Lu-PCBEH	10:10	CB	DIO,ODCB	0.92	0.58	0.36	0.19
		10:10	CB	ODCB	0.44	0.28	0.27	0.03
		10:10	ODCB	DIO	0.90	0.86	0.37	0.29
		10:10	ODCB	None	0.31	0.42	0.26	0.03
		12:15	ODCB	None	0.31	0.14	0.26	0.01
		15:12	ODCB	None	0.60	0.24	0.27	0.04
Plex B	Lu-PCBEH	8:8	CB	CINp	0.05	0.20	0.25	0.00
		10:8	CB	None	0.02	0.09	0.28	0.00

Table 4: Plex A/C₇₀-PCBM device fabrication matrix

Spin, RPM	Time, s	Dry Condition	Pre-Anneal, °C/min	Post-Anneal, °C/sec	V _{oc}	J _{sc}	FF	PCE
600	75	Close PD	120/10	160/30	0.66	5.96	0.35	1.38
500	200	Open PD	none	None	0.67	5.46	0.34	1.23
500	200	Open PD	120/10	None	0.66	4.81	0.35	1.10
500	200	Close PD	120/10	None	0.67	5.76	0.34	1.32

Table 5: Impact of post annealing on Plex A/C₇₀-PCBM devices based on sequential thermal treatments

Spin, RPM	Time, s	Dry Condition	Pre-Anneal, °C/min	Post-Anneal, °C/time	V _{oc}	J _{sc}	FF	PCE
600	75	Closed PD	120/10	160/30sec	0.66	6.03	0.35	1.39
				120/10min	0.66	6.05	0.34	1.37
				175/20min	0.59	4.47	0.37	0.99
500	200	Open PD	None	None	0.67	5.53	0.34	1.26
				160/30sec	0.68	5.80	0.35	1.37
				175/20min	0.66	6.18	0.38	1.56
500	200	Open PD	120/10	None	0.66	4.90	0.35	1.14
				160/30sec	0.67	5.53	0.34	1.27
				120/10min	0.67	5.55	0.33	1.26
				175/20min	0.61	5.27	0.36	1.15
500	200	Closed PD	120/10	None	0.66	5.83	0.35	1.35
				160/30sec	0.67	5.61	0.34	1.28
				120/10min	0.67	5.70	0.34	1.29
				175/20min	0.60	4.42	0.35	0.93

Table 6: Effect of spin coating speed and time for Plex A/C70-PCBM (10:10, no thermal treatment, no additive)

RPM	Spin Time		
	75s	100s	200s
600	0.65V		0.65V
	6.18mA/cm ²		5.62mA/cm ²
	0.34		0.32
	1.36%		1.15%
700		0.66V	0.65V
		6.14mA/cm ²	5.45mA/cm ²
		0.34	0.3
		1.39%	1.07%
800		0.67V	
		5.81mA/cm ²	
		0.34	
		1.32%	

Table 7: Effect of spin coating speed and time for Plex A/Lu-PCBEH (10:10, no thermal treatment, no additive)

RPM	Spin Time		
	75s	150s	200s
500			0.88V
			0.38mA/cm ²
			0.3
			0.10%
600	0.54V	0.88V	
	0.42mA/cm ²	0.42mA/cm ²	
	0.26	0.3	
	0.06%	0.11%	
700	0.50V		0.67V
	0.43mA/cm ²		0.35mA/cm ²
	0.27		0.26
	0.06%		0.06%

The absence of good short circuit currents and fill factors for both Plex A and Plex B polymers over a range of process conditions strongly suggests a more fundamental incompatibility between the donor and acceptor energy levels. Therefore, in parallel to device testing at Luna, the HOMO levels of the materials were measured at Plextronics using their AC2 system to confirm the selection of these polymers as appropriate for pairing with Lu-PCBEH. The resulting HOMO level and band gap data confirmed both Plex A and especially Plex B **do not** align favorably with Lu-PCBEH, Figure 7. Efforts were therefore refocused on polymer selection and ongoing test matrices were not completed. No further testing of Plex A and Plex B polymers was planned.

Table 8: Effect of additives on Plex A/Lu-PCBEH 10:10 blend in ODCB

% Additive	Spin, RPM	Time, sec	Dry Condition	Pre-Anneal, °C/min	Post-Anneal, °C/sec	V_{oc}	J_{sc}	FF	PCE
2% DIO	600	150	Closed PD	120/10	160/30	0.91	0.39	0.26	0.09
	500	200	Closed PD	None	none	0.88	0.09	0.19	0.02
	600	75	Closed PD	120/10	160/30	0.93	0.22	0.31	0.06
6% DIO	600	150	Closed PD	120/10	160/30	0.94	0.75	0.39	0.28
	500	200	Closed PD	None	none	0.88	1.12	0.42	0.42
	600	75	Closed PD	None	none	0.59	0.74	0.30	0.13
10% DIO	600	150	Closed PD	120/10	160/30	0.94	0.70	0.41	0.27
	500	200	Closed PD	120/10	160/30	0.92	1.15	0.42	0.44
	600	75	Closed PD	120/10	160/30	0.94	0.72	0.41	0.28
15% DIO	500	200	Closed PD	None	none	0.92	1.12	0.43	0.44
	500	300	Closed PD	None	none	0.92	1.12	0.42	0.43
	2000	60	Closed PD	None	none	0.74	0.74	0.40	0.22
2% ODT	500	200	Closed PD	None	none	0.94	0.93	0.34	0.17
	600	75	Closed PD	None	none	0.47	0.47	0.25	0.03

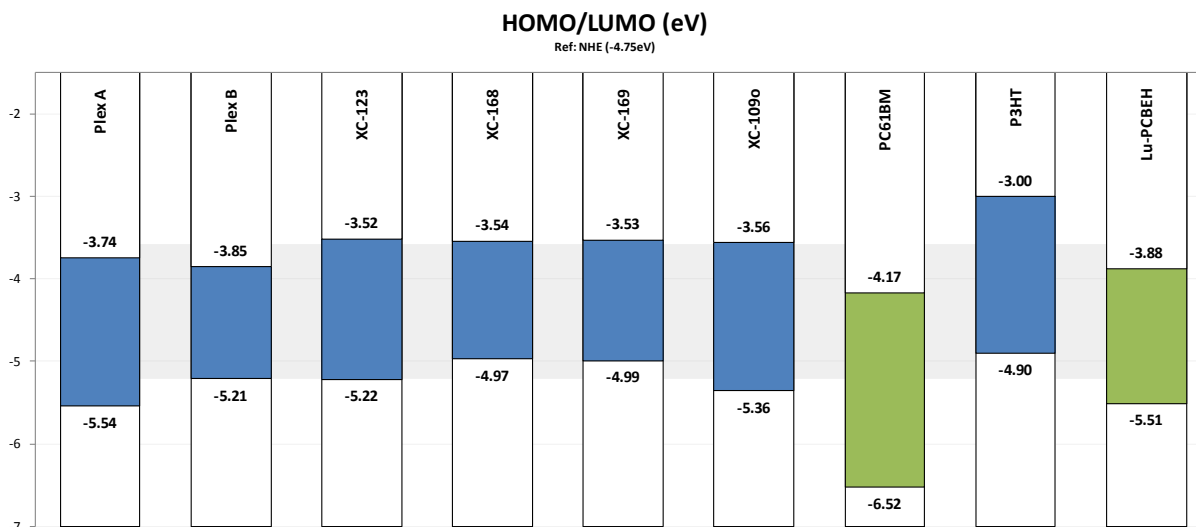


Figure 7: HOMO/LUMO comparison for donors and acceptors based on UPS measurements (except P3HT which is based on electrochemical measurement)

With the determination that new polymers were essential for program success, Plextronics reviewed their internal data for alternative polymers better aligned with Lu-PCBEH. Four new polymers were selected for evaluation. Samples were received September 10th and evaluation of these new polymers was conducted at Luna. Testing of these new polymers included blend ratio, solvent variations including additives, spin coating conditions, and thermal annealing conditions. The extent of this testing was limited by the availability of the polymer.

One additional polymer for a total of five polymers (XC-109, XC-123, XC-145, XC-168, XC-169) was received from Plextronics after the initial round of testing. These polymers were selected based on HOMO/LUMO levels more compatible with the Lu-PCBEH acceptor. Figure 7 shows the electronic energy levels of six of the polymers along with acceptors. Data for XC-145 was not available. The energy difference between the LUMO of these new polymers and that of Lu-PCBEH is greater than 0.30 eV, an energy difference believed to be significant in overcoming the binding energy of the excitons and allowing charge transfer. The HOMO levels of the new polymers should still provide a significant advantage in V_{oc} when paired with the Lu-PCBEH compared to C₇₀-PCBM due to the larger energy difference between the HOMO of the polymers and the LUMO of Lu-PCBEH.

Device Fabrication and Characterization

Initial devices fabricated with XC-123 and Lu-PCBEH spun cast from the blend in ODCB showed particles and suggested a solubility issue. Efforts to filter the polymer through a 1 μ m filter were unsuccessful as the filter quickly clogged. Despite aggregates the devices produced a V_{oc} in the 0.80-1.0 V range but the highest measured current of 1.3 mA/cm² and low fill factors (0.3-0.39) led to conversion efficiency of only 0.46% for the best device. Further experiments with other solvents and additives were carried out in an attempt to better dissolve the polymer and improve film morphology. Use of CHCl₃ as an additive to the ODCB and other solvent systems such as 2%CN/CB and tri-chlorobenzene (TCB) slightly improved the solubility of the

polymer and yielded better looking films. While V_{oc} remained higher with these solvents J_{sc} was lower resulting in a decrease in cell efficiency (Table 9). Baseline devices were fabricated using C₇₀-PCBM and data are included for comparison. Further study of XC-123 with Lu-PCBEH and other derivatives were hampered by a limited quantity of the polymer.

Table 9: Device data for XC-123 with C₇₀-PCBM and Lu-PCBEH acceptors

Polymer XC-123							
Acceptor	Ratio (D:A)	Solvent	Additive	Voc (V)	Jsc (mA/cm ²)	FF	Eff
LuPCBEH	7:14	ODCB	---	0.89	1.31	0.39	0.46
LuPCBEH	10:10	ODCB	---	0.95	0.799	0.34	0.26
C70PCBM	7:14	ODCB	20% CHCl ₃	0.75	11.13	0.41	3.39
LuPCBEH	7:14	ODCB	20% CHCl ₃	1.01	1.05	0.37	0.4
C70PCBM	7:14	TCB	---	0.73	9.76	0.49	3.48
LuPCBEH	7:14	TCB	---	0.99	0.72	0.35	0.25
LuPCBEH	10:10	CB	2% ClNp	0.91	0.555	0.31	0.15
LuPCBEH	7:14	ODCB	50% CHCl ₃	0.89	0.711	0.34	0.22
LuPCBEH	10:10	ODCB	50% CHCl ₃	0.87	0.242	0.32	0.07
LuPCBEH	7:10	CHCl ₃	20% ODCB	0.98	0.6	0.32	0.19
LuPCBEH	7:14	CHCl ₃	20% ODCB	0.97	0.6	0.33	0.19

Devices prepared with XC-168 also suffered from limited solubility of polymer at higher loadings. Despite changes in solvent system, devices produced with the XC-168 polymer gave lower and varied V_{oc} . Coupled with low currents and fill factors, these devices showed PCE <0.26% as outlined in Table 10. Similar to devices made with the XC-168 polymer, those fabricated with XC-169 provided V_{oc} lower than typically observed with other polymers such as P3HT.

Table 10: Device data for XC-168 and XC-169 polymers blended with Lu-PCBEH and C₇₀-PCB M

Polymers XC-168 and XC-169								
Polymer	Acceptor	Ratio (D:A)	Sovent	Additive	Voc (V)	Jsc (mA/cm ²)	FF	Eff
XC-168	LuPCBEH	10:10	ODCB	---	0.41	1.01	0.28	0.12
XC-168	LuPCBEH	10:10	ODCB	4% DIO	0.67	1.27	0.31	0.26
XC-168	LuPCBEH	15:30	ODCB	---	0.52	1.1	0.29	0.17
XC-168	C70PCBM	15:30	ODCB	---	0.6	4.15	0.45	1.13
XC-168	LuPCBEH	10:10	CB	2% ClNp	0.67	1.19	0.31	0.25
XC-168	LuPCBEH	10:20	CB	2% ClNp	0.7	1.14	0.31	0.25
XC-169	LuPCBEH	15:30	ODCB	---	0.8	1.18	0.32	0.3
XC-169	LuPCBEH	10:10	ODCB	---	0.77	0.955	0.32	0.24

Devices fabricated with XC-109 and XC-145 gave the lowest PCE due primarily to very low current and in the case of XC-109, very low V_{oc} . In the case of XC-145 different solvent systems, additives, and ratios were studied in an attempt to influence morphology and increase currents. The use of additives and solvents other than ODCB had a negative impact on J_{sc} . Results are shown in Table 11.

Table 11: Device data for XC-109 and XC-145 polymers with Lu-PCBEH and C70-PCBM

XC-109 and XC-145								
Polymer	Acceptor	Ratio (D:A)	Solvent	Additive	Voc (V)	J _{sc} (mA/cm ²)	FF	Eff
XC-109	LuPCBEH	7:14	ODCB	---	0.41	0.333	0.28	0.04
XC-109	LuPCBEH	10:10	ODCB	---	0.12	0.234	0.25	0.01
XC-145	LuPCBEH	7:14	ODCB	---	1.02	0.32	0.37	0.12
XC-145	LuPCBEH	10:10	ODCB	---	0.93	0.19	0.3	0.05
XC-145	LuPCBEH	10:10	ODCB	2% DIO	0.82	0.07	0.27	0.01
XC-145	LuPCBEH	10:10	ODCB	2% ODT	0.85	0.05	0.28	0.01
XC-145	LuPCBEH	7:14	CB	2% ClNp	0.93	0.016	0.2	0.003
XC-145	LuPCBEH	10:10	CB	2% ClNp	0.96	0.035	0.24	0.008
XC-145	LuPCBEH	7:14	Xylene	---	0.05	0.07	0.23	0
XC-145	LuPCBEH	7:14	Xylene	2% ClNp	0.95	0.35	0.33	0.11
XC-145	LuPCBEH	7:14	Xylene	2% DIO	0.39	0.03	0.27	0
XC-145	C70PCBM	7:14	ODCB	---	0.73	10.26	0.46	3.47

Thermal Annealing

As seen from the above tables and results, solvent annealing (using additives and different solvents) was conducted with each of the polymers. Thermal annealing was also performed on devices made with each of the five newer polymers in an attempt to increase current, Table 12. Solvent annealing can influence morphology by altering phase separation, crystallinity, and interface development. However, experiments with thermal treatments at different steps in the device preparation process led to detrimental effects on current and overall PCE. Therefore solvent annealing was determined to be the best option to influence morphology. Ratios of donor and acceptor were also examined, but varying the concentration of the polymer was limited by its solubility (even at the lower concentration suggested by Plextronics, solubility of XC-123, for example, was very limited).

Table 12: Effect of thermal annealing for Plextronics' polymers blended with Lu-PCBEH

Effect of Thermal Treatment							
Polymer	Ratio	Solvent	Anneal	Voc (V)	Jsc (mA/cm ²)	FF	Eff
XC-123	7:14	20%CHCl ₃ /ODCB	none	0.97	0.98	0.36	0.34
	7:14	20%CHCl ₃ /ODCB	post 160C/30s	1.02	0.52	0.34	0.18
XC-168	15:30	ODCB	none	0.52	1.1	0.29	0.17
	15:30	ODCB	post 160C/30s	0.46	0.874	0.25	0.1
	10:10	2%ClNp/CB	none	0.67	1.19	0.31	0.25
	10:10	2%ClNp/CB	pre 120C/10m	0.41	0.849	0.26	0.09
XC-169	15:30	ODCB	none	0.76	1.19	0.3	0.27
	15:30	ODCB	post 160C/30s	0.76	0.915	0.28	0.2
	10:10	ODCB	none	0.77	0.955	0.32	0.24
	10:10	ODCB	post 160C/30s	0.73	0.689	0.28	0.14
XC-109	7:14	ODCB	none	0.18	0.312	0.26	0.01
	7:14	ODCB	pre 120C/10m	0.04	0.23	0.25	0.002
XC-145	10:10	2% DIO/ODCB	none	0.82	0.07	0.27	0.01
	10:10	2% DIO/ODCB	pre 120C/10m	0.11	0.08	0.25	0

The continued observation of low current density for the different polymer/acceptor blends led to examination of possible causes for poor PCE. One possible reason for the low currents is poor film morphology: gross phase separation or poor miscibility that prevents exciton dissociation at the donor/acceptor interface or hinders mobility of charge carriers to the electrode. Another possible cause is mismatch of electronic energy levels and the subsequent lack of energy to drive exciton dissociation and efficient electron transfer. Morphology was studied by Plextronics using AFM and optical microscopy. Photoluminescence spectroscopy and time-resolved microwave conductivity measurements were carried out at NREL in an attempt to determine if poor device performance was due to free carrier generation and/or inefficient charge transfer.

Film Morphology and AFM

Four devices fabricated at Luna were submitted to Plextronics for AFM study comparing films prepared from two polymers, XC-123 and XC-168. For each polymer, two substrates were chosen that represented the best and worst overall PCE for that polymer (Table 13).

For each of the XC-169:Lu-PCBEH blended films, AFM shows significant phase separation greater than 250nm which could account for poor device performance, Figures 8 and 9. The less homogeneous and optimized mixing of polymer with the Lu acceptor molecule would lead to donor/acceptor (D/A) interfaces that limit charge transfer and interrupt pathways for charge transport. However, each of the films prepared with XC-123 displayed a more intimate mixing of polymer and acceptor with phase separation on the order of 10nm, Figures 10 and 11. According to Plextronics' experience with these polymers, domain sizes 10-50 nm in the heterojunction is characteristic of higher performing OPV devices.

Table 13: Device performance for samples prepared for morphology study.

Films Submitted for AFM Study								
Substrate Id	Polymer	Ratio (D:A)	Solvent	Additive	Voc (V)	Jsc (mA/cm ²)	FF	Eff
2603	XC-123	7:14	ODCB	--	0.89	1.31	0.39	0.46
2609	XC-123	10:10	ODCB	CHCl ₃	0.87	0.242	0.32	0.07
2557	XC-169	10:10	ODCB	--	0.47	0.554	0.28	0.07
2562	XC-169	15:30	ODCB	--	0.8	1.18	0.32	0.3

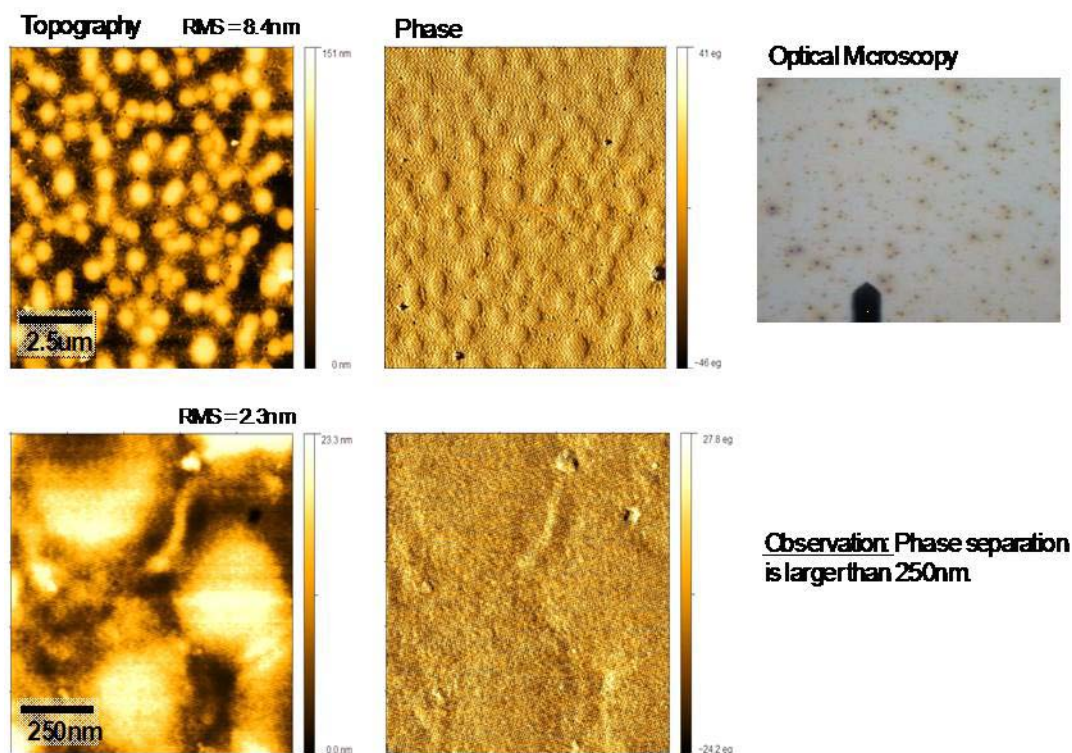


Figure 8: AFM images of film 2557 cast from XC-169+LuPCBEH blend.

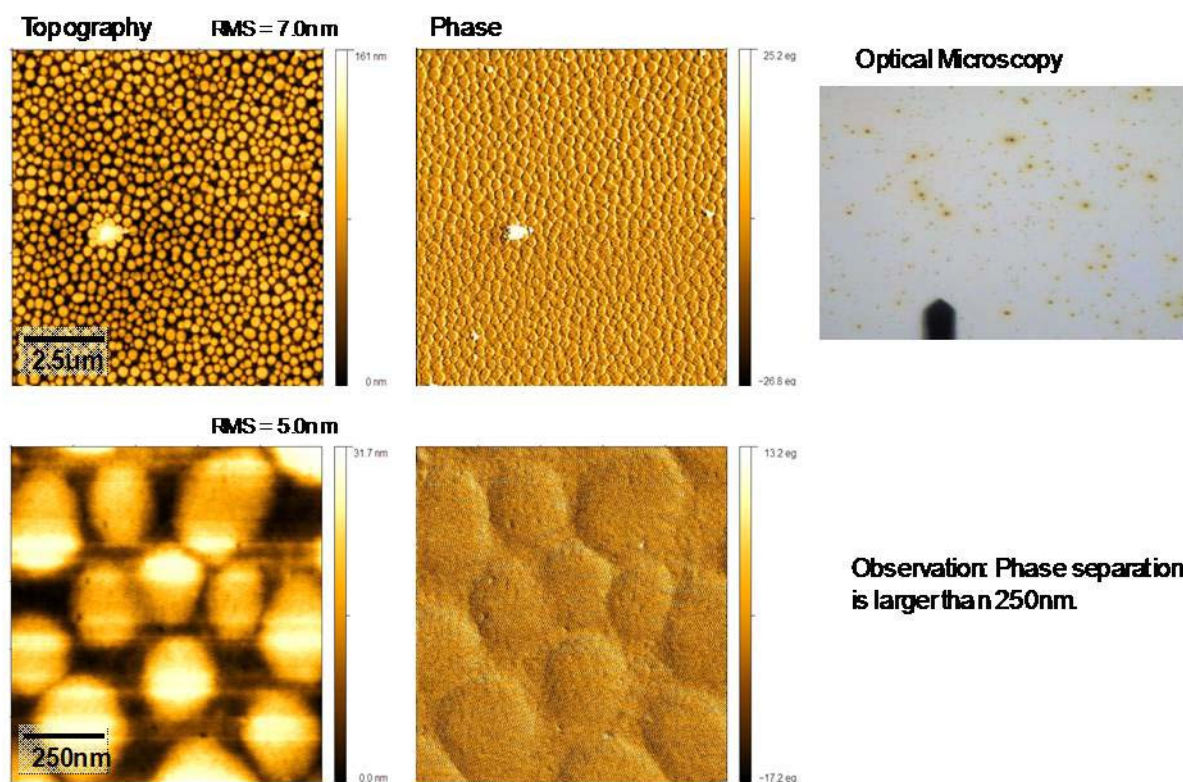


Figure 9: AFM images of film 2562 cast from XC-169+LuPCBEH blend.

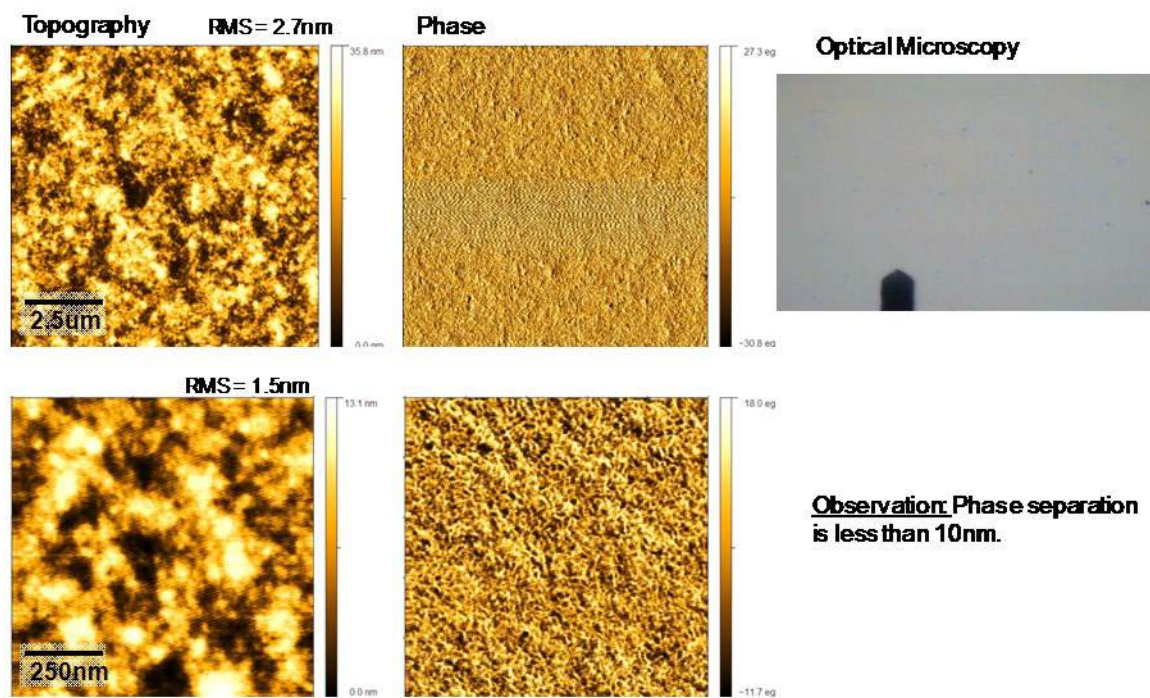


Figure 10: AFM images of film 2603 cast from XC-123+LuPCBEH blend.

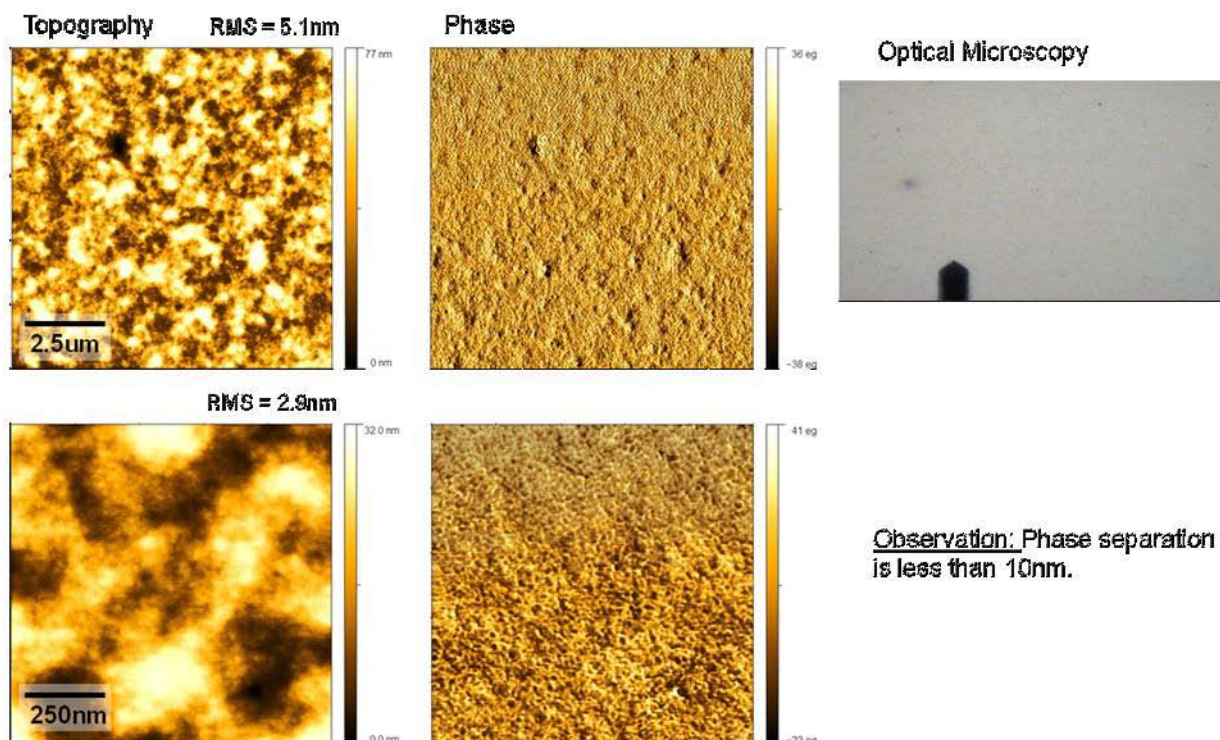


Figure 11: AFM images of film 2609 cast from XC-123+LuPCBEH blend.

Despite the smaller domain sizes and better morphology of the XC-123 films, the currents observed were unusually low and suggest factors other than active layer morphology contributed to the low performance. Other methods were investigated to understand charge generation and transfer in the different polymer/Lu-PCBEH blended films.

Photoluminescence Spectroscopy

Using an in-house Odyssey infrared imaging system, we compared near infrared fluorescence of a P3HT/Lu-PCBEH film with films prepared using Lu-PCBEH and the polymers from Plextronics. Films spun with P3HT blended with C₇₀-PCBM and Lu-PCBEH showed quenching of fluorescence indicating efficient exciton dissociation (Figure 12). Those consisting of Plextronics' polymers and C₇₀-PCBM also displayed quenching; however, these polymers paired with Lu-PCBEH showed significant fluorescence (Figure 13), suggesting inefficient exciton dissociation and/or charge transfer.

A more sophisticated luminescence study employing time-resolved luminescence spectroscopy was conducted by Dr. Darius Kuciauskas at NREL. Photoluminescence spectra were recorded after laser excitation and corresponding luminescence lifetimes were measured for the polymer only films (Figure 14). Lifetimes were estimated to be 16-70 ps for the different polymers, with the XC-109 polymer having a luminescent lifetime of 221 ps. According to Dr. Kuciauskas, these excited state lifetimes are certainly long enough for charge transfer to occur since transfer in photovoltaic devices occurs on the femtosecond scale. It should be noted that P3HT had one of the shortest lifetimes at 16 ps (a polymer that combined with Lu-PCBEH has provided devices

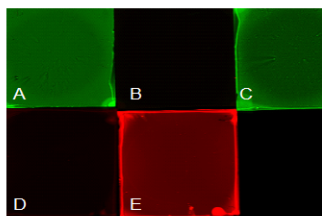
with $J_{sc} > 10 \text{ mA/cm}^2$) while the devices fabricated with XC-109 and its longer lifetime have generated very low $J_{sc} \sim 0.3 \text{ mA/cm}^2$. However, flash photolysis data raised questions concerning charge separation in the different polymer-acceptor systems. Transient absorption data for the blended films, Figure 15, was very similar to that displayed by the polymer only films, Figure 16. Excitation was at 532 nm, kinetics were measured at wavelengths 500-750 nm as shown in the graph. These wavelengths gave the strongest signals for each sample. Excitation intensity was the same for all measurements (15 mW, 10 Hz laser repetition rate, beam diameter about 5 mm). All signals were negative (“- ΔOD ” is shown) due to polymer ground-state absorption bleaching. Amplitudes of transient absorption signals depend not only on concentration of absorbing species, but also on the extinction coefficient of each polymer. Therefore, ΔOD signal amplitude cannot be used for comparing concentrations between different samples. Black horizontal lines indicate “baseline” before the laser flash at $\sim 250 \mu\text{s}$. All samples have long-lifetime non-single-exponential transients. The slower components have lifetime of $> 1 \text{ ms}$ for all samples.

As Dr. Kuciauskas commented, since charge separation is not occurring in polymer-only films, then the long lifetime bleaching signal, Figure 16, is the result of another process and the similar signal observed for the blended films cannot be attributed to efficient charge separation.

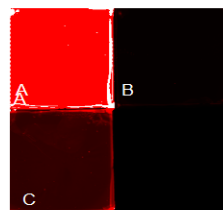


A = P3HT, B = P3HT:C70PCBM, C = P3HT:LuPCBEH

Figure 12: Near infrared images of A) neat P3HT; B) P3HT blended with C70-PCBM, and C) P3HT blended with Lu-PCBEH.



A = XC-168, B = XC-168:C70PCBM, C = XC-168:LuPCBEH
D = XC-123:C70PCBM, E = XC-123:LuPCBEH



A = XC-145, B = XC-145:C70PCBM, C = XC-145:LuPCBEH

Figure 13: Near IR fluorescence detection neat polymer films and blends paired with Lu-PCBEH and C₇₀-PCBM (reference). Left – A) XC-168, B) XC-168:C70-PCBM, C) XC-168:Lu-PCBEH, D) XC-123:C70-PCBM, E) XC-123:Lu-PCBEH. Right – A) XC-145, B) XC145:C70-PCBM, C) XC-145:Lu-PCBEH

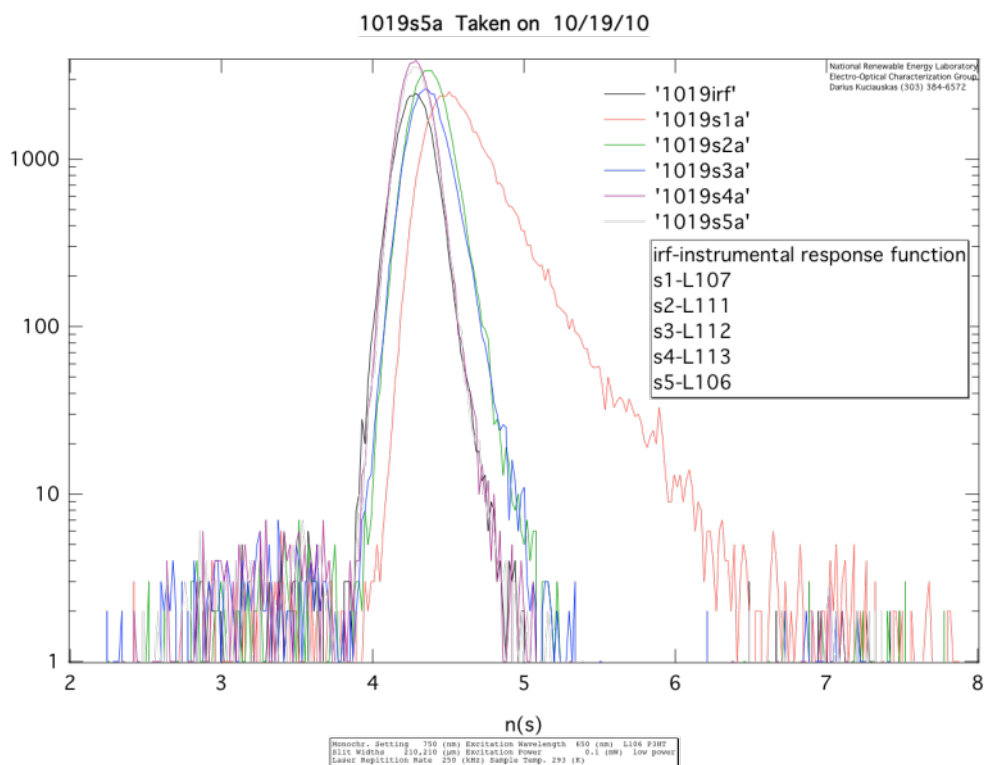


Figure 14: Luminescence lifetime of polymer films: s1-L107=XC-109, s2L111=XC-168, s3-112=XC-169, s4-L113=XC-123, s5-L106=P3HT. Excitation wavelength = 650nm, 200 fs laser pulses at excitation power = 0.1mW.

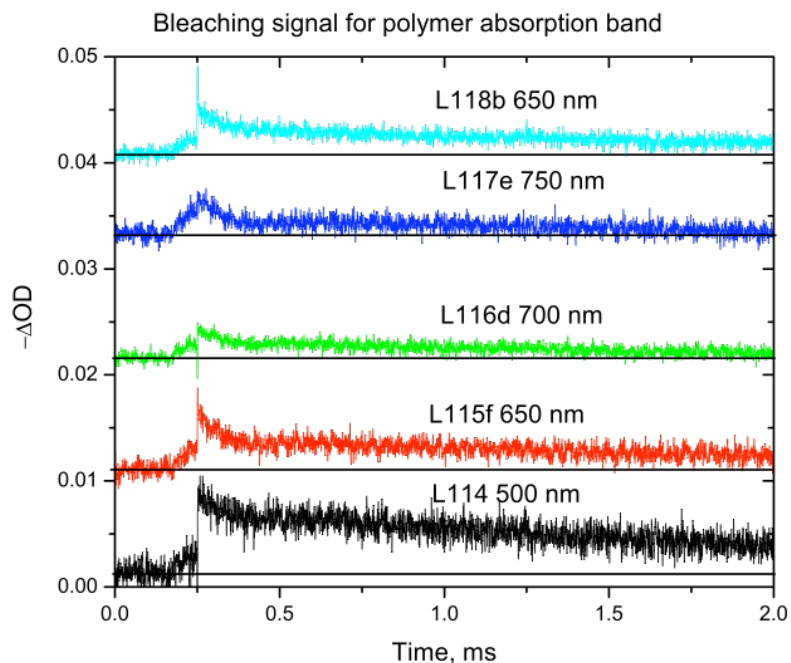


Figure 15: Transient absorption (flash photolysis) data for polymer/fullerene films. Absorption kinetics are vertically offset for clarity. Key: L114 = P3HT+LuPCBEH, L115 = XC-109+LuPCBEH, L116 = XC-168+LuPCBEH. L117 = XC-169+LuPCBEH.

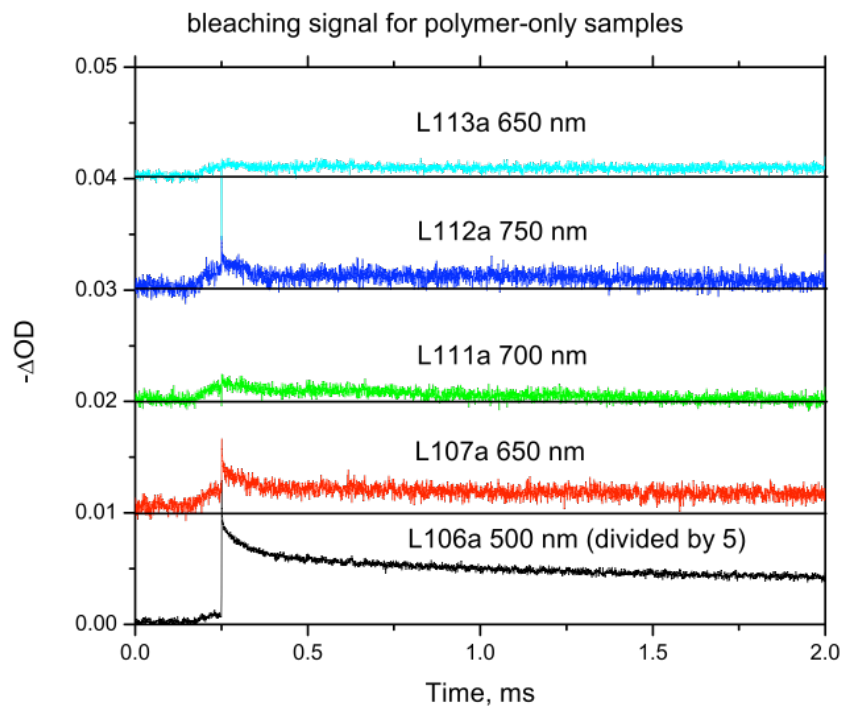


Figure 16: Transient absorption (flash photolysis) data for polymer-only films—very similar to that observed for polymer/fullerene films in Figure 15. Key: L06 = P3HT, L07 = XC-109, L111 = XC-168,

Samples of polymer films and blended films (except XC-168 because supply was consumed) were submitted to Dr. Nikos Kopidakis at NREL for more in-depth photoconductivity study using time-resolved microwave conductivity measurements. These photoconductivity measurements (Figure 17) show that films prepared with Lu-PCBEH and Plextronics' polymers suffer much lower free carrier generation and mobility compared to P3HT:Lu-PCBEH blended film. As Dr. Kopidakis noted, this data suggests that low current and device performance can be attributed to the diminished free carrier generation rather than film morphology.

According to the photoconductivity data, XC-123:Lu-PCBEH shows slightly better carrier generation and mobility compared to the other polymers which is demonstrated in the measured J_{sc} and overall efficiency of a device fabricated with XC-123 (Table 14). Despite the better domain sizes and phase separation in XC-123:Lu-PCBEH films (as seen earlier in AFM images), the free carrier generation and mobility remain substantially low suggesting an unfavorable match in orbital energy. In the case of XC-169:Lu-PCBEH where previous AFM showed phase separation on the order of 250+nm, the low carrier generation and mobility could be attributed to poor morphology. While AFM is useful in examining domain sizes and separation, it is limited to the topography of films which prevents a more detailed study of the morphology within the bulk heterojunction layer. In fact, for these polymer:Lu-PCBEH films, the molecular structures of the donor and acceptor may not provide the ideal interface where excitons can dissociate nor a percolating network for carrier mobility.

Quantum yield (ϕ) \times sum of mobilities ($\Sigma\mu$) vs. light intensity ($F_A I_0$): comparison between blends and pure donors

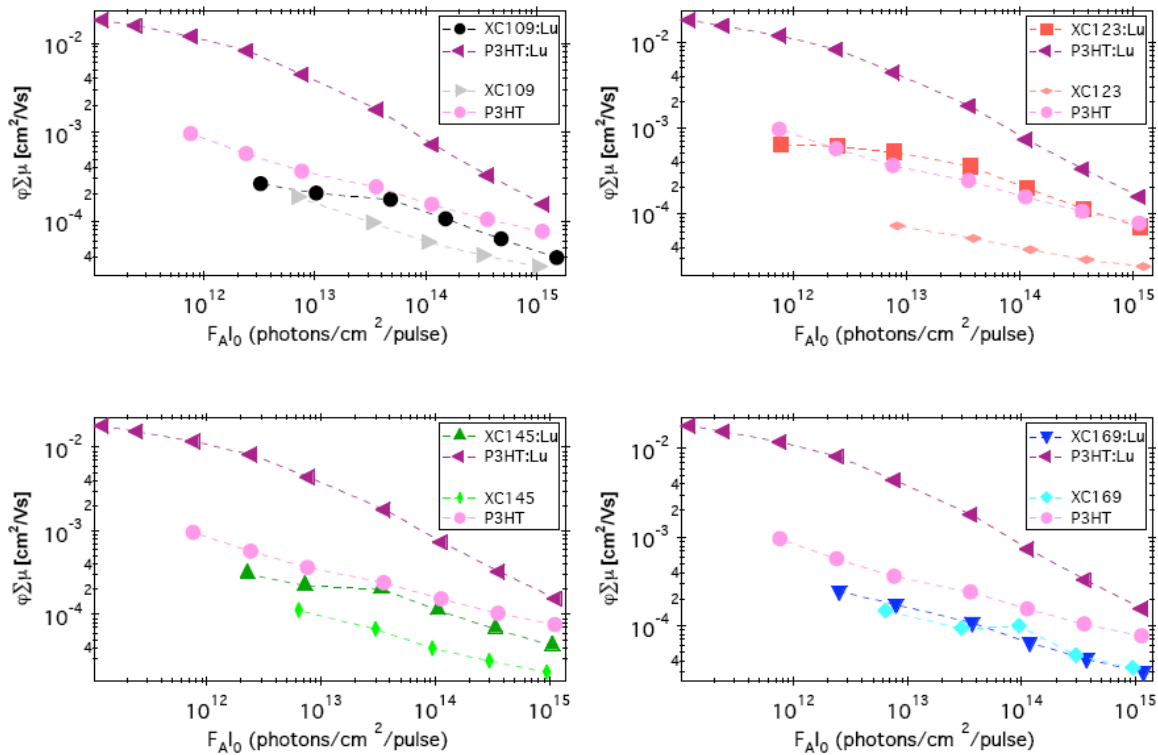


Figure 17: Time-resolved microwave conductivity data comparing blended films to pure donor films. P3HT is included for reference.

Table 14: Performance data for devices used in the TRMC study

Devices Prepared From Blended Solutions Used in Films Submitted for TRMC Study							
Polymer	Acceptor	Ratio (D:A)	Solvent	V_{oc} (V)	J_{sc} (mA/cm ²)	FF	Eff
P3HT	PCBEH	10:10	ODCB	0.81	9.727	58	58
C-109	PCBEH	7:14	ODCB	0.21	0.346	25	02
C-123	PCBEH	7:14	20%CHCl ₃ /ODCB	1.01	1.052	37	4
C-145	PCBEH	7:14	ODCB	1.02	0.321	37	12
C-169	PCBEH	15:30	ODCB	0.69	1.038	3	21

Additional Derivatives Tested as Acceptors

An effort was made to synthesize different derivatives for testing with Plextronics' polymers. The different side chain functional groups were intended to provide a better "fit" and interaction with the polymers, through better miscibility and/or pi interactions, for example. The actual chemical structures or formulas of the Plextronics' polymers were not known, so understanding how interaction between the functionalized derivatives and polymer could be enhanced was hindered. Nevertheless, different derivatives were employed in a continuous effort to impact the current generated by the devices. Results of this testing are shown in Table 15.

Table 15: Device performance data for different fullerene and Trimetasphere derivatives.

Blends of Polymers with Different Fullerene Derivatives								
Polymer	Acceptor	Ratio	Solvent	Voc	Jsc	FF	Eff	Note
XC-168	LuPCBTMH	15:30	ODCB	.19-.52	.84-.857	.26-.28	.04-.12	some particles, poor solubility of polymer
	LuPCBIsoB	15:30	ODCB	---	---	---	---	lots of particles
	C70 mono acetophenone	15:30	ODCB	---	---	---	---	lots of particles
P3HT	LuPCBTMH	10:10	2%CN/CB	0.82	10.451	0.56	4.81%	
P3HT	LuPCBBEG	10:10	2%CN/CB	0.80	9.955	0.59	4.70%	
P3HT	LuPCBIsoB	10:10	ODCB	0.62	6.176	0.34	1.30%	Particles
XC-169	LuPCBTMH	15:30	ODCB	.31-.61	.80-.82	.26-.29	.07-.15	particles
	LuPCBBPy	15:30	ODCB	---	---	---	---	lots of particles, poor solubility of D&A?
XC-109	LuPCBTMH	7:14	ODCB	0.1	0.27	0.25	0.01	uniform film
	LuPCBIsoB	7:14	ODCB	0.04	0.2	0.24	0	uniform film
	LuPCBBEG	7:14	ODCB	0.19	0.3	0.25	0.01	aggregates/poor solubility of LuPCBBEG
	LuPCBBPy	7:14	ODCB	0.02	0.1	0.3	0	aggregates/poor solubility of LuPCBBPy
	C70 mono biphenyl	7:14	ODCB	0.26	0.6	0.27	0.04	uniform film
XC-145	Lu diamide	7:14	ODCB	0.7	0.0707	0.25	0.01	uniform film
XC-123	Lu diamide	7:14	20%CHCl ₃ /ODCB	0.84	0.295	0.3	0.08	particles, polymer solubility
P3HT	Lu diamide	10:10	2%CN/CB	0.60	1.270	0.40	0.30%	
P3HT	Lu diamide	10:10	ODCB	0.59	1.378	0.42	0.35%	

Synthetic approach to develop a library of novel OPV acceptor materials

C₆₀ and C₇₀ fullerenes are carbon cages composed of 60 and 70 carbons, respectively, with set electronic properties. Trimetasphere carbon nanomaterials (TMS) are cages composed of 80 carbons and contain a metal-nitride cluster in the interior which influences the electronic properties of these electron acceptor molecules (Figure 18). The unusual electronic properties of these TMS fullerenes have opened up a new frontier of research in the development of molecular electronics.

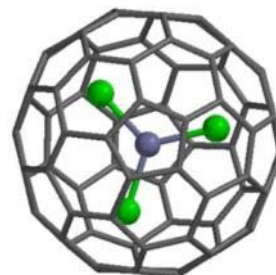


Figure 18: Trimetasphere carbon nanomaterials, M₃N@C₈₀ where the metals (M = Sc, Y, Er, Lu, Gd) are green, and the nitrogen is blue.

In the production of Trimetaspheres nanomaterials, empty cage fullerenes such as C₆₀ and C₇₀ are obtained as by-products. Therefore, Luna has at hand all the raw materials necessary to create a library of fullerene acceptors. Matching the molecular orbitals of both the acceptor (fullerene based) and donor components (conducting polymers) in OPV is as important as securing an optimum morphology of the blend to maximize the photovoltaic effect.

In this project, an exploratory investigation was initiated regarding the effect of structural modification of an acceptor molecule on the tuning of molecular orbital energies. The primary goal was to find the best matching acceptor units for the polymers which were supplied by collaborators in an effort to obtain photoconversion efficiencies above 7%. In addition, development of new derivatives to test with poly(3-hexylthiophene), P3HT, continued, since higher photoconversion efficiencies may still be obtained with this polymer. The potential of blends using TMS derivatives with P3HT has yet to be maximized. *Just last year efficiencies in the 4.5% range were obtained and this year performance has improved to >5.4 % with V_{oc} values of 0.84 V.* However, devices with V_{oc} values up to 0.93 V have been fabricated, which suggest that optimization of the morphology of the bulk heterojunction has not yet been achieved with this polymer.

It is reasonable to expect efficiencies in the 7.5% range with the only commercially available conducting polymer (P3HT) when optimum fabrication conditions are achieved with TMS-derivatives. This achievement would be significant since the production of novel polymers is much more costly.

Synthesis of C₇₀ and TMS derivatives with desired electronic properties

Acceptor materials based on Trimetaspheres

Companies such as Konarka, Solarmer, and Plextronics are the leading developers of conducting donor polymers in the world, and they have successfully integrated their polymers with either 1-(3-methoxycarbonyl)propyl-1-phenyl-[6,6]C₆₁, C₆₀PCBM, or 1-(3-methoxycarbonyl)propyl-1-phenyl-[6,6]C₇₁, C₇₀PCBM, into the active layer of their solar devices. These empty cage fullerene acceptors (Figure 19) have been employed from the beginning of the OPV technology in 1995 and have had no matching competition until now.

The advantage in organic photovoltaics of TMS-PCBX (see examples in Figure 20) over C_{60} -PCBM is based on one of our recent discoveries: *Luna can control the electronic properties of TMS species by enclosing different metals and by selective functionalization of the carbon cage. This allows engineering of their molecular orbitals to better match the electronic properties of the donors and thereby enhance the V_{oc}* (Figure 21).

The V_{oc} advantage originates on the less negative LUMO orbital of the TMS species in the eV scale compared to the C_{60} and C_{70} fullerenes (Figure 21). A significant amount of energy is lost during the electron transfer from the donor to the acceptor molecule due to the large energy offset between their lowest unoccupied molecular orbitals (LUMOs). There has been a burst of development of low band-gap polymers which also

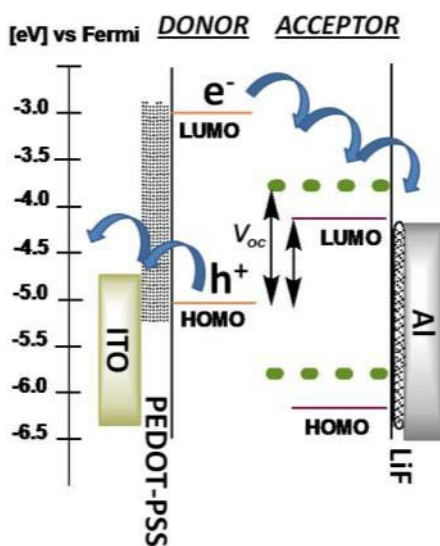


Figure 21: Electron transfer from the HOMO of the donor (orange for P3HT) to the LUMO of the acceptor (burgundy for C_{60} PCBM or C_{70} PCBM). The TMS LUMO lies higher (green dots), and thus it is energetically more efficient with higher V_{oc} .

brings a V_{oc} advantage due to the lowering of the HOMO/LUMO band-gap compared to P3HT. Thus these perform at higher efficiencies compared to P3HT combined with C_{60} / C_{70} -PCBM. Such is the case of the record setting polymer from Solarmer [Y. Liang, Z. Xu, J. Xia, S. T. Tsai, Y. Wu, G. Li, C. Ray, and L. Yu, *Advanced Materials* 22, E135 (2010); C. Hsiang-Yu, H. Jianhui, Z. Shaoqing, L. Yongye, Y. Guanwen, Y. Yang, Y. Luping, W. Yue, and L. Gang, *Nature Photonics* 3, 649 (2009)].

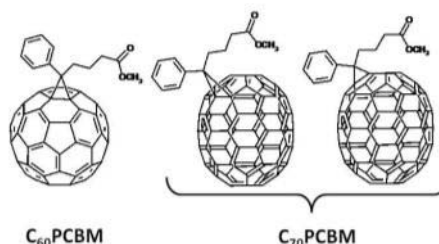


Figure 19: C_{60} and C_{70} derivatives employed as acceptors materials in OPVs.

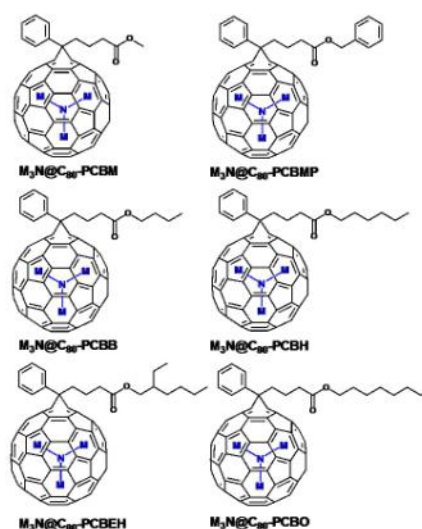


Figure 20: TMS-PCBX ([6,6]-phenyl C_{81} butyric acid X ester) family: TMS-PCBM (M, methyl ester); TMS-PCBMP (MP, benzyl ester); TMS-PCBB (B, butyl ester); TMS-PCBH (H, hexyl ester); TMS-PCBEH (EH, ethyl hexyl ester); and TMS-PCBO (O, octyl ester).

The molecular orbitals of our TMS derivatives, however, can be tuned to match an array of donor polymers. Substitution of the metal in the endohedral cluster is one method to control the LUMO of the TMS-PCBM-type derivatives, as shown in Table 16. The first reduction (LUMO) of C₆₀PCBM occurs at -1.22 V while that of Sc₃N@C₈₀-PCBM is more negative (higher LUMO in eV scale) at -1.36 V. When the metals of the cluster are substituted for lutetium, these derivatives display an even higher LUMO at -1.50 V (Lu₃N@C₈₀-PCBM and other esters such as PCBMP, PCBH, and PCBEH). On the other hand, the LUMO lies in between that of the scandium and the lutetium derivatives when the metal in the endohedral cluster is yttrium (at -1.46 V for Y₃N@C₈₀-PCBH and Y₃N@C₈₀-PCBEH). The more negative the LUMO of the acceptor, the lesser the gap to the LUMO of P3HT which promotes a larger V_{oc} and a more efficient electron transfer.

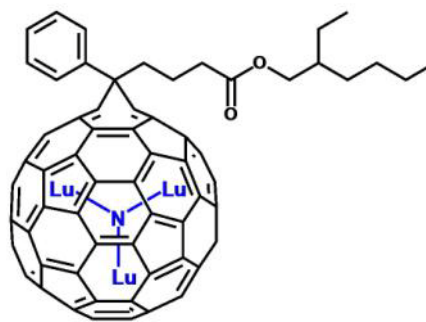


Figure 22: 1-(3-(2-ethyl)hexylcarbonyl)propyl-1-phenyl-[6,6]Lu₃N@C₈₁ or LuPCBEH.

Noticeably, any changes in the side group X of the TMS-PCBX derivatives *DO NOT* influence the energies of the HOMO/LUMO levels. However, this side group triggers changes in their physical properties which play an important role in the morphology of the bulk heterojunction.

As with C₆₀, pristine TMS solubility is too low for solution processing. Thus, we modified the TMS structure via derivatization that resembles C₆₀-PCBM. This modification improved TMS solubility and has given an additional advantage due to a higher LUMO of this type of methano derivatives compare to the pristine TMS (see Table 16). One of the best donor-acceptor combinations was obtained with the 2-ethyl-hexyl ester derivative (Figure 22), Lu₃N@C₈₀-PCBEH, which performed with highest efficiency in devices with poly-3-hexylthiophene polymer (P3HT). This branched side group not only improves the solubility of the TMS derivative, but enhances its miscibility in the donor polymer. The miscibility factor has proven crucial in device fabrication since it prevents microscale phase separation which interferes with charge generation and electron mobility.

Evidently, the introduction of an aromatic unit into the TMS side group with the 4-phenyl-butyl ester, Lu₃N@C₈₀-PCBBP, to induce π - π^* interactions led to the highest observed fill factors but modest efficiencies. Thus, the aromatic unit seems to have enhanced the interactions of not only acceptor-acceptor but acceptor-donor components in the polymer blend.

Table 16: Redox potentials (V vs Fc+/Fc) for the first oxidation (HOMO) and first reduction (LUMO) processes measured by OSWV in 0.05 M n-Bu₄NPF₆/o-OCB.

	E _{p, ox(1)} V	E _{p, red(1)} V
C₆₀-PCBM	+1.132	-1.220
Sc₃N@C₈₀	+ 0.559	-1.31
Sc₃N@C₈₀-PCBM	+ 0.505	-1.368
Sc₃N@C₈₀-PCEH	+0.506	-1.360
Lu₃N@C₈₀	+0.635	-1.424
Lu₃N@C₈₀-PCBM	+0.556	-1.510
Lu₃N@C₈₀-PCBMP	+ 0.552	-1.500
Lu₃N@C₈₀-PCBH	+0.564	-1.500
Lu₃N@C₈₀-PCBEH	+0.558	-1.502

Initially, we proposed the incorporation of additional aromatic elements into the structure of the $\text{Lu}_3\text{N}@\text{C}_{80}\text{-PCBX}$ derivative such as a thiophene-based element, which was expected to improve the interaction with thiophene-based polymers while maintaining interactions with other acceptor components. In addition, we were to incorporate a molecular unit, such as a branched alkyl group, to ensure not just solubility but miscibility as well. We quickly found though that aromatic elements in the X portion of the molecule induced aggregation which was detrimental to the morphology of the OPV devices. Therefore we searched for alternative structural designs.

New TMS derivatives of the PCBX type

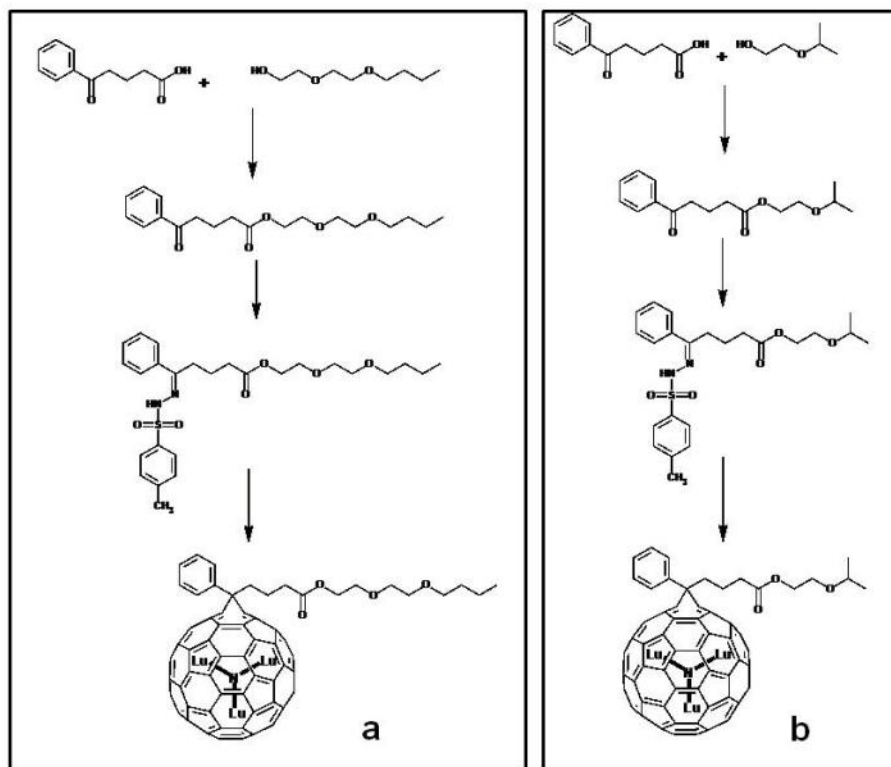


Figure 23: Reaction protocol for the synthesis of the ethoxy-TMS derivatives.

In an effort to prevent aggregation, two new X elements were employed. These elements contained polyethylene glycols which have been used in previous studies to disrupt aggregation forces between porphyrins derivatives. X consisted of either a 2-isopropoxyethyl ester or a 2-(2-ethoxyethoxy)ethyl ester (Figure 23). These derivatives, however, did not give rise to higher efficiencies. When additives such as diiodooctane are employed in OPV device processing, an increase in short circuit current J_{sc} and an improvement in fill factor are observed. This effect has been attributed to the improvement in morphology, but more specifically to the suppression of holes and electron recombining into long lived low lying electronic state with triplet spin signature [Di Nozzo, D., Aguirre, A., Shahid, M., Gevaerts, V. S., Meskers, S. C. J., Janssen, R. A. J. *Adv. Mater.* **2010**, 22 (38), 4321–4324].

Based on this premise, we decided to try to create derivatives that would contain a moiety capable of impeding the formation of these triplet states. The addition of surfactants such as ethylene glycol derivatives with different chain lengths have been employed to control the size and shape of nanoparticles composed of meso-substituted tetracarboxyphenyl porphyrins ($\text{H}_2\text{P}(\text{CO}_2\text{H})_4$). These porphyrins form microstructures with significant excited triplet states. However, in the presence of ethylene glycols, these microstructures dissociate into assemblages in the nano-range which undergo quenching processes of the triplet states [Sandanayaka, A. S D., Araki, Y., Wada, T., Hasobe, T. *J. Phys. Chem. C* **2008**, 112, 19209-19216]. Thus, we introduced ethylene glycol units into the X component of the Lu-PCBX derivatives (Figure 23).

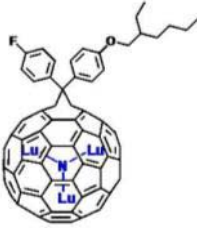
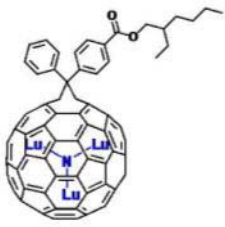

Unfortunately, there was not enough time to build a significant library of ethylene glycol-TMS derivatives to find if our hypothesis was correct. The tri-dimensionality of the fullerene unit may require longer ethylene glycol chain lengths or the addition of several ethylene glycol units into the structure to minimize aggregation and allow for nano-assemblages of the acceptor components in the bulk heterojunction to enhance the short circuit current and fill factor in the OPV devices.

TMS derivatives with new linkers

The need to explore new acceptor materials for OPVs has become essential in the advent of the plethora of low band-gap polymers being produced. Most of these polymers continue to be tested with C_{60} -PCBM and C_{70} -PCBM and many do not perform as expected.

We believe that instead of coming up with many new polymers and employing the same acceptors, scientist should concentrate on tweaking the electronic and physical properties of both the donor and acceptor materials to improve efficiencies. Therefore, we have concentrated on building a library of acceptors to improved active layer materials for organic solar cells through advanced molecular design.

Table 17: Redox potentials (V vs Fc+/Fc) for the first oxidation (HOMO) and first reduction (LUMO) processes measured by OSV in 0.05 M n-Bu₄NPF₆/o-OCB.

	HOMO	LUMO
	+ 0.552 V	- 1.448 V
	+ 0.588 V	- 1.484 V
	+ 0.508 V	- 1.468 V

We have focused on finding the effect of new linkers on the electronic properties of the acceptor molecules. As described above, the PCBX linker on Lu-TMS gives rise to lower LUMO and the X factor only influences physical properties such as morphology. We were intrigued by new findings which assert that the V_{oc} does not solely depend on the molecular orbitals of donor/acceptor couples. For example, Prof. Martin has recently shown that in some cases *the morphology of the OPV device does influence the V_{oc}* in an unexpected manner. While his biphenyl-methano derivatives of C_{60} (Figure 24) display the same reduction potential as C_{60} -PCBM (same LUMO levels), devices fabricated with this novel derivative exhibited higher V_{oc} with P3HT than does C_{60} -PCBM [A. Sánchez-Díaz, M. Izquierdo, S. Filippone, N. Martin, and E. Palomares, *Advanced Functional Materials* 20, 2695 (2010)]. Therefore, *in some cases there is much more to the molecular orbital matching than just comparing the energy levels of the donor/acceptor materials. Thus, the need for exploring new molecular designs becomes obvious.*

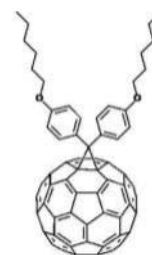


Figure 24: Biphenyl methano derivative of C_{60} .

The addition of a biphenyl-methano linker onto TMS molecules had never been explored before. In this project, we designed this synthesis and created a series of Lu-TMS derivatives with subtle modifications of this biphenyl linker to test for any control of the electronic properties of such derivatives. As mentioned early, the electronic properties of TMS-PCBX derivatives do not respond to changes of the X group. We were thus surprised to see significant influence of any variations in the biphenyl design on the electronic properties of the material. In addition, these variations of the biphenyl unit also dictated the physical properties such as solubility. For example, the Lu-biphenyl-methano derivative was sufficiently insoluble to preclude its use in OPVs.

On the other hand, the 4-ethylhexyl ester derivative depicted in Figure 25a proved to be more soluble, but still not enough for processing without visible aggregation. The 3,4-di-ethylhexylamide (Figure 25b) derivative however proved to be soluble enough, but its electronic properties contrasted significantly with other

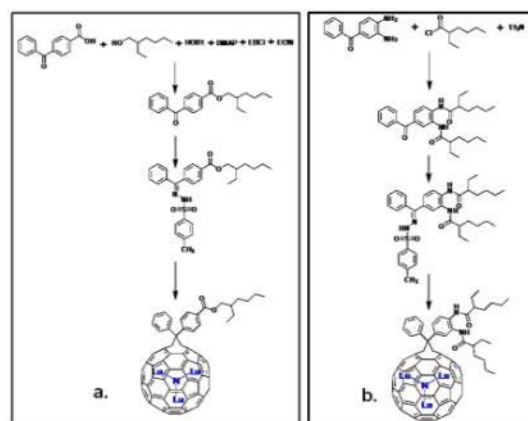


Figure 25: Biphenyl methano derivative of $Lu_3N@C_{80}$ (a. 4-ethylhexylester and b. 3,4-di-ethylhexylamide).

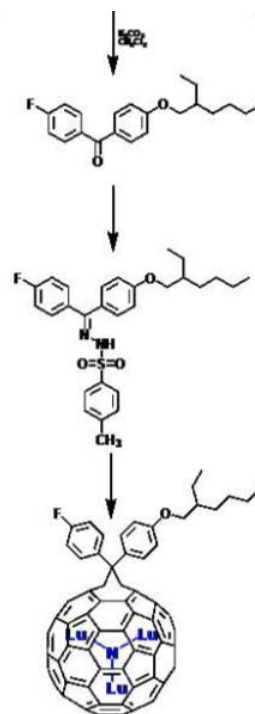


Figure 26: Biphenyl-methano derivative of $Lu_3N@C_{80}$ (4-ethylhexylether-4'-fluoro).

biphenyl-methano derivatives as shown in Table 17.

The effect of the substituents of the aromatic units of the biphenyl-methano linker on the electronic properties of TMS derivative is impressive. For example the (4-ethylhexylether-4'-fluoro)biphenyl-methano derivative of $\text{Lu}_3\text{N}@\text{C}_{80}$ shown in Figure 26 oxidizes at a similar potential to $\text{Lu}_3\text{N}@\text{C}_{80}$ -PCBX (Lu-PCBX) and reduces at a potential only 50 mV less than these PCBX derivatives which resemble the reduction potentials of the $\text{Y}_3\text{N}@\text{C}_{80}$ -PCBX group. The (4-ethylhexylester) biphenyl-methano derivative of $\text{Lu}_3\text{N}@\text{C}_{80}$ reduces at closer potentials to the Lu-PCBX example but oxidizes at higher energies such as $\text{Y}_3\text{N}@\text{C}_{80}$ -PCBX. Then the (3,4-diethylhexylamide) biphenyl-methano molecule also reduces at similar potentials but requires less energy to oxidize which closely resembles the $\text{Sc}_3\text{N}@\text{C}_{80}$ -PCBX derivatives. Therefore, the substituents on the phenyl groups can alter the molecular energies of these TMS derivatives in a manner that looks like the nature of the internal metal is substituted.

Further investigation into these types of derivatives will provide the key to assemble a library of TMS derivatives for OPVs. Additional derivatives were attempted but the initial reactions did not work.

Acceptor materials based on empty cage fullerenes

Recently a mixture of bis-adducts of C_{60} , Diels-Alder bis-indene derivatives (Figure 27) have been reported to display a V_{oc} of 0.84 V in combination with P3HT [G. Zhao, Y. He, and Y. Li, *Advanced Materials*, 22, (39), 4355–4358 (2010). Y. He, H.-Y. Chen, J. Hou, and Y. Li, *Journal of the American Chemical Society* **132**, 1377 (2010). Y. He, H.-Y. Chen, J. Hou, and Y. Li, *Journal of the American Chemical Society* **132**, 5532 (2010)].

Initially, these molecules performed at 5.4 % efficiency and upon improvement of the morphology of the OPV devices, efficiencies of 6.5 % have been reached in the lab setting. These efficiencies have not been yet verified by independent certification laboratory such as NREL or Newport Corporation.

The V_{oc} advantage of this material originates from the second adduct on the fullerene cage. It is well known that the less sp^2 character the fullerene has, the higher the LUMO of the material. Thus the second addend induces a more negative reduction potential. The reported reduction potential of these bis-indene derivatives is at -1.07 V while C_{60} -PCBM occurs at -0.88 V vs Ag/Ag⁺ reference electrode. Under our conditions, the first reduction of C_{60} -PCBM takes place at -1.22 V vs Fc/Fc⁺. Consequently, the first reduction of the bis-indene mixture should be at -1.41 V vs the latter reference electrode. In comparison, the $\text{Lu}_3\text{N}@\text{C}_{80}$ -PCBX monoadducts (-1.50 V vs Fc/Fc⁺) still have an advantage of ~100 mV to the bis-indene derivatives (Table 16). Therefore, higher efficiencies should be expected with

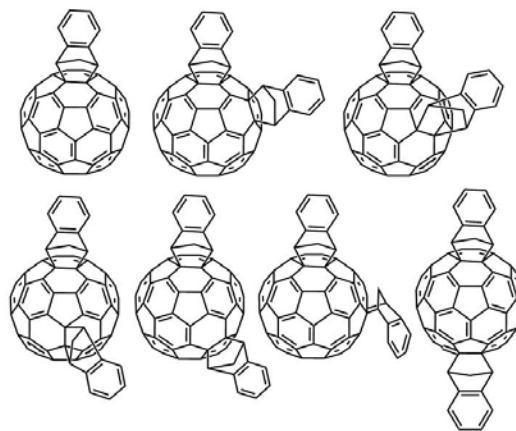


Figure 27: Possible regioisomers in the mixture of C_{60} -bis-indene derivatives.

these TMS derivatives than those achieved with these C₆₀-bisadducts after the appropriate morphology is obtained.

Interestingly, not every type of C₆₀-bisadduct will work for OPVs. In the design of acceptors, a balance between the number of addends and the preservation of the fullerene surface is needed because the lesser the fullerene character, the lesser the electron transport across the fullerene nanophase. For example, the bis-adduct of the PCBM type (C₆₀-bis-PCBM) has not reach higher than 4.5 % efficiencies even if their reduction potential is almost as negative as the bis-indene derivative [M. Lenes, G. J. A. H. Wetzelaer, F. B. Kooistra, S. C. Veenstra, J. C. Hummelen, and P. W. M. Blom, *Advanced Materials* **20**, 2116 (2008). M. Lenes, S. W. Shelton, A. B. Sieval, D. F. Kronholm, J. C. Hummelen, and P. W. M. Blom, *Advanced Functional Materials* **19**, 3002 (2009)]. It is believed that the multiple PCBM addends interfere with formation of the most effective morphology for electron transport. We should note that tris-adducts of C₆₀ would have even a more negative LUMO, but the addends will impede the electron transport due to steric hindrance.

The success of the bis-indene derivatives, however, may not have an easy transition into the commercial market since their production is not cost effective. The mixture of regioisomers of C₆₀-bis-indenes requires a demanding purification protocol which could be even more costly than production of TMS-mono-adduct derivatives, a fact not mentioned in the published work. Based on our knowledge of fullerene chemistry we anticipated such purification problems and therefore, we followed the synthetic procedure as described in the literature to verify our suspicions. Our results clearly show that a mixture of unreacted C₆₀, C₆₀-mono-indene, and C₆₀-bis-indenes are obtained which display such close polarities that simple column chromatography with silica gel would not only consume tremendous man power because repetitive columns are required, but the yield of the desired product would be low, and the materials cost (silica gel, solvent) would be an obstacle to bring these acceptors to commercial use. In addition, these derivatives are quite insoluble which makes processing even more difficult.

As fullerene chemists, we know that the polarity of regioisomeric bis-adducts is very similar when the species in question is C₇₀ instead of C₆₀ because the addition takes place at the poles of the C₇₀ cage (Figure 28). Thus the purification of a mixture of C₇₀-bis-indene isomers is expected to involve conditions not as rigorous as with the C₆₀ mixture. The polarity of the mixture of C₇₀-bis-adducts is much different from that of C₇₀ or the C₇₀-mono-adduct, thus their isolation is more feasible. Recently, the same researchers who developed the bis-indene C₆₀ derivatives published their finding on the mixture of C₇₀-bis-indene molecules [Y. He, G. Zhao, B. Peng, and Y. Li, *Advanced Functional Materials* **20**(19), 2010, 3383–3389]. As we had expected, they made note of the ease of purification when the modified fullerene was C₇₀ instead of C₆₀. The initial efficiencies with the C₇₀ bis-indene acceptors reached 5.9% which is expected to increase

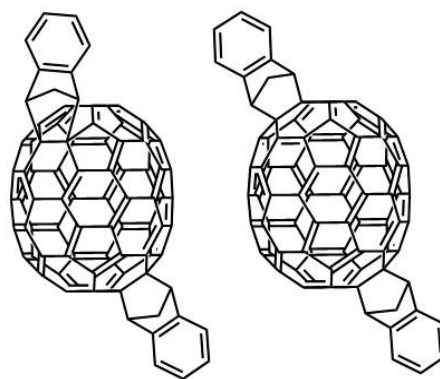


Figure 28: Example of indene-bis-adducts of C₇₀. These are mainly characterized by addition at the poles of the C₇₀ elongated cage.

as the device fabrication is optimized but so far the improvement has not been reported. Furthermore, the authors have not reported the difficulty to get these materials in solution.

In-house, we have developed the expertise to functionalize many different fullerenes, including C_{70} , in our Medical Division and have comprehensive knowledge on the reactivity of most fullerene species. In addition, C_{70} has proven to have an advantage in OPVs over C_{60} since its absorption expands over the visible range which in turn enhances the absorption properties of the active layer in an OPV device [W. S. Shin, Y. M. Hwang, W. W. So, S. C. Yoon, C. J. Lee, and S. J. Moon, *Molecular Crystals and Liquid Crystals* **491**, 331 (2008). F. B. Kooistra, V. D. Mihailetschi, L. M. Popescu, D. Kronholm, P. W. M. Blom, and J. C. Hummelen, *Chemistry of Materials* **18**, 3068 (2006)]. In addition, C_{70} is a by-product in the production of TMS materials, as mentioned early, and thus, we have at hand the basic materials to develop an acceptor library with all possible electronic and physical characteristics.

Based on difficulty achieving acceptable current, it was decided to include a study of novel C_{70} acceptors as a means to meet the 7% PCE goal. This study was to explore the electronic properties of both mono- and bis-adducts of a particular linker and modify the side groups to tune their physical properties as was discovered for the TMS molecules described above. In addition, the study investigated different substituents to enhance the solubility of C_{70} derivatives to mitigate problems in device processing.

The mono-adducts of C_{70} are expected to have similar reduction potentials to C_{70} PCBM (similar LUMO energy), and the bis-adduct will display a more negative LUMO, but questions remained regarding the effect of the adduct on morphology and the affect on V_{oc} .

Based on Prof. Martin's findings on the improved V_{oc} of the biphenyl-methano C_{60} derivatives, it was decided to pursue both mono-adduct and bis-adducts of the biphenyl linker with the C_{70} fullerene. The bis-adducts of C_{70} are expected to have an advantage in LUMO over the C_{70} -PCBM as mentioned earlier for the C_{60} derivatives.

The biphenyl linker also resembles the aromatic indene adduct which may help organize the packing in the nanophase of the acceptor material due to π - π supramolecular interactions and thus allow for a more seamless transport of current.

Concurrently, similar derivatives were prepared with methyl-phenyl-methano linker to explore new options. Figure 29 depicts the first derivatives obtained with these methano adducts. The mono- and bis-(4-benzylether)biphenyl-methano derivatives (Figure 29a) displayed significant aggregation while the methyl-(4-benzoylate)phenyl materials (Figure 29b) displayed a more

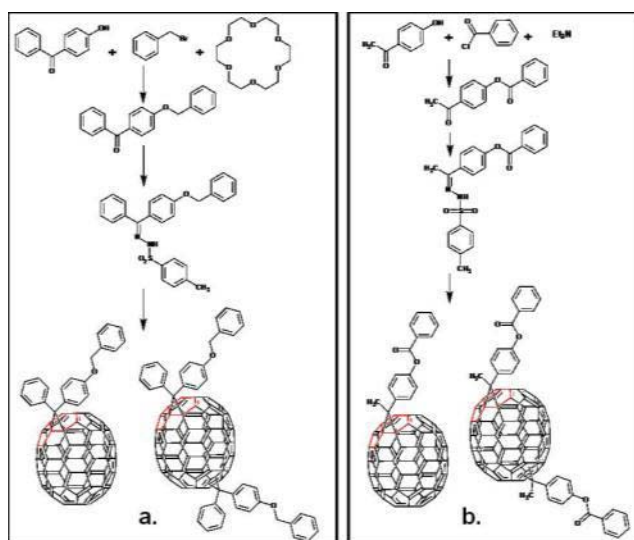


Figure 29: Biphenyl-methano and methy-phenyl-methano derivatives synthesized in this project.

soluble character. Figure 30 describes four additional methyl-phenyl-methano derivatives which displayed significant solubility in organic solvents.

When the electronic properties of these molecules were studied by electrochemistry, a clearer picture was perceived of the effect substituents exert on the linker. Empty cage fullerenes seem not to be as sensitive as TMS molecules and therefore the substituent effect was more subtle. However, some interesting findings were made.

As expected (Table 18), the LUMO of bis-adducts of C_{70} became more negative compared to the mono-adducts except for the methyl-(2,3,4-tri(2-ethyl)hexoyl)phenyl-methano material (Figure 30b). The electronic effect of the tri-hexanoyl substituents compared to the mono-hexanoyl substitute (Figure 30a) induced a very modest effect when going from the mono- to the bis-adduct. All other substituents behaved as expected, giving rise to a more negative LUMO upon the addition of the second addend. The former effect has not been reported before, which raises the question of what other electronic effects have not been explored with empty cage fullerenes.

Further development of these empty cage fullerene derivatives will be necessary to discover the requirements to tune both electronic and physical properties. Such developments were not able to be accomplished during this program due to time limitations.

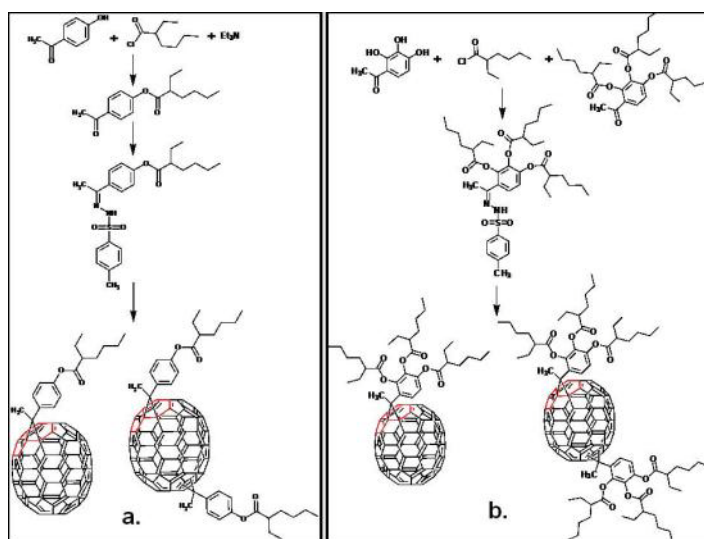



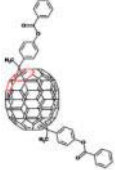
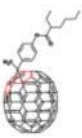
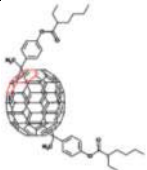
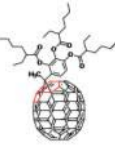
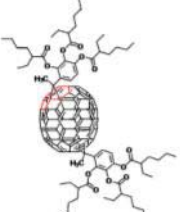


Figure 30: Additional methyl-phenyl-methano derivatives prepared and studied.

The bis-adduct C_{70} derivatives were synthesized for use with the P3HT polymer while the mono-adduct products were isolated for study with some of Plextronics polymers. Initial testing of the C_{70} compounds showed solubility limit issues especially with the mono-adduct derivatives, but additional experiments with different solvents and loadings were not completed due to time constraints. Despite the limited solubility, some of these new derivatives (C_{70} bis-acetophenone, C_{70} bis-EH, and C_{70} bis-tri-EH) yielded $J_{sc} \sim 3\text{-}5 \text{ mA/cm}^2$ in P3HT-based OPV devices. These initial results suggest further optimization and study would be beneficial.

Table 18: Redox potentials (V vs Fc+/Fc) for the first oxidation (HOMO) and first reduction (LUMO) processes measured by OSWV in 0.05 M n-Bu₄NPF₆/o-OCB.

	HOMO	LUMO
	+ 0.868 V	-1.220
	> + 0.96 V	- 1.312 V
	> +1.0 V	- 1.232 V
	> +0.86 V	- 1.304 V
	+ 1.024 V	- 1.244 V
	+ 0.868 V	- 1.320 V
	+ 1.090 V	- 1.168 V
	+ 1.080 V	- 1.200 V

Additional Polymers Tested as Donors with Lu-PCBEH

While research efforts were focused on Plextronics' polymers as suitable donors with LuPCBEH in bulk heterojunction devices, the opportunity became available to test the functionalized TMS with polymers synthesized by Dr. Wei You's group at the University of North Carolina-Chapel Hill. Researchers at UNC-CH have achieved efficiencies as high as 7.8% PCE with their unique molecularly engineered polymers paired with C₆₀-PCBM. The electrochemical data for these new polymers (Table 19) indicates an energy difference >0.3 eV between LUMO of polymer and LUMO of the functionalized Lu-TMS, an offset that should provide efficient exciton dissociation. Additionally, the low HOMO energies should still yield a significant V_{oc} advantage, and in fact, devices fabricated with the PBnDT-DTffBT polymer produced V_{oc} greater than one volt (Table 20) while the PBnDT-DTPyT and PBnDT-fTAZ polymers generated open circuit voltages of 0.92-0.99mV. However, the overall performance remained below 0.50% PCE due to low currents and fill factors.

Table 19: Electrochemical data for UNC-Chapel Hill polymers

Electrochemical Data		
Polymer	HOMO (eV)	LUMO (eV)
PBnDT-DTffBT	-5.54	-3.33
PBnDT-DTPyT	-5.47	-3.44
PBnDT-fTAZ	-5.36	-3.05

Table 20: Device performance for UNC-Chapel Hill polymers blended with Lu-PCBEH

Devices Fabricated with UNC-CH Polymers and Lu-PCBEH							
Polymer	Ratio (D:A)	Solvent	Voc (V)	Jsc (mA/cm ²)	FF	Eff	Anneal
PBnDT-DTPyT	10:10	ODCB	0.99	0.429	0.38	0.16	no
PBnDT-DTPyT	10:10	2% CN/CB	0.86	0.449	0.32	0.12	no
PBnDT-DTPyT	10:10	2% CN/CB	0.62	0.179	0.29	0.032	yes
PBnDT-DTffBT	10:10	ODCB	1.05	0.695	0.44	0.32	no
PBnDT-DTffBT	10:10	ODCB	1.06	0.207	0.34	0.075	yes
PBnDT-DTffBT	8:16	ODCB	0.97	0.922	0.51	0.46	no
PBnDT-DTffBT	10:10	2% CN/CB	1.02	0.687	0.36	0.26	no
PBnDT-DTffBT	10:10	2% CN/CB	1.04	0.221	0.31	0.07	yes
PBnDT-fTAZ	12:24	TCB	0.92	0.581	0.44	0.24	no

Conclusions

Baseline performance for Luna's functionalized lutetium Trimetasphere, Lu-PCBEH, blended with P3HT exceeded program expectations with a certified PCE of 4.89% in a 0.12cm² area device. Use of Lu-PCBEH in place of C₆₀-PCBM surpassed expectations with a demonstrated V_{oc} advantage of 260mV based on devices fabricated using similar processing conditions and architecture.

Research did not yield a bulk heterojunction OPV device with 7% PCE using Plextronics' polymers and Lu-PCBEH. While the significant V_{oc} advantage was observed with several of Plextronics' polymers, the current generated was consistently low and problematic.

One possible explanation for the low current is the energy offset of the LUMO levels between the polymer and acceptor. For the P3HT and Lu-PCBEH system, which can produce current density greater than 10 mA/cm² and PCE greater than 5%, the LUMO difference is substantially greater than that offered by the Plextronics' polymers tested (reference Figure 7). Additionally, it is unclear how the energy difference in the HOMO levels of both donor and acceptor affect charge mobility. Can similar HOMO energy levels lead to traps and poor carrier mobility? Most OPV research utilizes the common acceptor C₆₀-PCBM with a much deeper HOMO level compared to Lu-PCBEH. Examining the affect of HOMO level for both donor and acceptor material has not received adequate attention to address this concern.

Another factor that may account for the limited current is the nanomorphology within the bulk heterojunction layer. The molecular structure of polymer and the size and/or structure of the functionalized TMS play a critical role in the compatibility, arrangement, and interaction between donor and acceptor. These molecular differences can lead to limited or less than optimal interface sites for exciton dissociation and may limit pathways for electron transport.

Many new acceptor molecules were synthesized and a new pathway for tuning of HOMO/LUMO levels was demonstrated. However, testing of these new acceptors was restricted due to supply limitations for low band gap polymers. Significant potential exists to pursue these new acceptor molecules in combination with appropriately engineered polymers that may lead to significant improvement in device performance.

Additional polymers were provided by Dr. Wei You at UNC-Chapel Hill. Dr. You is eager to work with Luna and is confident a polymer better matched to Lu-PCBEH or a modified acceptor based on TMS technology can be designed and synthesized. The design/development of polymers engineered specifically for TMS derivatives focusing on its functionalized character and size as well as energy levels has been proposed via *grants.gov* and is awaiting review. This proposal has support of many academic and commercial interests that have each provided letters of support for the continued development of TMS-based acceptors.